UNIVERSITY OF CALIFORNIA
RIVERSIDE

Environmental Chamber Study of Atmospheric Chemistry and Secondary Organic Aerosol Formation Using Cavity Enhanced Absorption Spectroscopy

A Thesis submitted in partial satisfaction
of the requirements for the degree of

Master of Science

in

Chemical and Environmental Engineering

by

Yingdi Liu

August 2011

Thesis Committee:
Dr. David R Cocker III, Chairperson
Dr. Akua Asa-Awuku
Dr. Jingsong Zhang

The Thesis of Yingdi Liu is approved:

Committee Chairperson

University of California, Riverside

ACKNOWLEDGEMENTS

This thesis could be done successfully is due to many people who helped me. First, I am deeply and sincerely grateful to my master program advisor, Dr. David Cocker, for his insightful guidance, continuous support, inspiring discussion, constant encouragement and kind understanding throughout my master program. Meanwhile, I would like to thank to my PhD program advisor, Dr Jingsong Zhang who is smart and considerate. Without his support, it would be impossible for me to take another major or study in other department.

In addition, I am grateful to Dr Akua Asa-Awuku, Dr Paul Ziemann, Dr Roger Atkinson and Dr William Cater for their priceless advices for my research work. It is lucky for me to have these many great scientists to help me when I meet any kinds of difficulties during my research work. I also appreciate all the professors in both chemistry and chemical engineering departments who taught me. I learned the real science in UC – Riverside, which build up my solid background of science.

Thirdly, I would like to thank to all of my labmates and group members, including James Hargrove, David Medina, Yu Song, Xiaochen Tang, Ping Tang, Shunsuke Nakao and Gookyoung Heo. This work would not have been possible without the contributions of my fellow researchers and funding agencies, and I gratefully acknowledge their contributions.

Finally, I can not thank enough for my parents, Qiang Liu and Jixian Liu, for their patience and support as I pursue my degrees and my dream, and for the fact they gave me their love and my life.

ABSTRACT OF THE THESIS

Environmental Chamber Study of Atmospheric Chemistry and Secondary Organic Aerosol Formation Using Cavity Enhanced Absorption Spectroscopy

by

Yingdi Liu

Master of Science, Graduate Program in Chemical and Environmental Engineering
University of California, Riverside, August, 2011
Dr. David R. Cocker, Chairperson

Air pollution and global climate change are important environmental issues that affect our society. Deeper understanding of atmospheric chemistry is required to understand these problems and to develop effective control strategies. Environmental chambers have been used for the past few decades to study atmospheric chemistry and investigate processes leading to secondary pollutant formation. This thesis work provides two different high sensitivity real time cavity enhance absorption spectroscopy (CEAS) instruments to detect NO_3 radical and NO_2/ glyoxal for environmental chamber study. These CEAS instruments can monitor these species with high sensitivity (in sub-ppb concentrations), with good selectivity, and with high spatial resolution in real time and in situ.

Environmental chamber studies using CEAS instruments include NO_3 behavior and reaction kinetics between NO_3 and amine; sources and sinks for oxides of nitrogen (NO_x) in the atmospheric photooxidation reactions; glyoxal uptake by secondary organic aerosol

(SOA) under dry and humid conditions and glyoxal formation from the photooxidation of aromatic and isoprene. These studies provide insightful data in atmospheric processes and lead to a better understanding of the atmospheric system, which will eventually extend to environmental policy.

This thesis is only a part of my research work. For more information about my other work, including cavity ring down spectroscopy studies for peroxy radical, aerosol optical extinction, transparent thin and time of flight mass spectrometry studies for the initial steps of ozone and alkenes reaactions, please refer to my PhD thesis in Chemistry department, UC-Riverside.

Table of Content

List of Figures

List of Tables

Chapter 1 Introduction

Air pollution and global climate change are important environmental problems and issues that affect our society. The composition and chemistry of the atmosphere are important for many reasons, primarily because of the interactions between the atmosphere and living organisms. The composition of the Earth's atmosphere has been changed by human activity; some of these changes are harmful to human health, crops and ecosystems. Examples of the problems include acid rain, photochemical smog and global warming. To understand first and to control next these problems require deeper understanding of atmospheric chemistry, which seeks to reveal the causes of these problems and to evaluate the possible solutions and government policies.

The troposphere is the region of the Earth's atmosphere in which we live and into which chemical compounds are generally emitted as a result of human activities. Emissions of oxides of nitrogen (NO_x), volatile organic compounds (VOCs) and sulfur compounds (including SO_2 and reduced sulfur compounds) lead to a complex series of chemical and physical transformations which result in such effects as the formation of ozone in urban and regional areas (National Research Council, 1991) as well as in the global troposphere, acid deposition, and the formation of secondary particulate matter through gas/particle partitioning of both emitted chemical compounds and the atmospheric reaction products of VOCs, NOx, SO_2 and organosulfur compounds[1].

Major urban areas have experienced pollution from the formation of tropospheric ozone through photochemical reactions. VOC play an important role in the formation of

tropospheric ozone because of their formation of peroxyl radicals (RO_2), which convert NO to NO_2:

$$HO_2 + NO \rightarrow OH + NO_2$$

$$RO_2 + NO \rightarrow RO + NO_2$$

NO_2 is then photolyzed by sunlight to yield a singlet oxygen, which reacts with molecular oxygen to produce ozone (O_3):

$$NO_2 + h\nu \rightarrow NO + O\left(^3P\right)$$

$$O\left(^3P\right) + O_2 \xrightarrow{M} O_3$$

An important oxidant that initiates peroxyl radical formation from VOC's and drives daytime chemistry in the atmosphere is the hydroxyl radical (OH). Similarly, the major oxidation species of hydrocarbons, typically alkenes, at night is the nitrate radical (NO_3)[2]. NO_3 is formed by the reaction of NO_2 and ozone:

$$NO_2 + O_3 \rightarrow NO_3 + O_2$$

Overall, NO_x play a crucial role in atmospheric chemistry since they affect ozone removal and production as well as mixing ratios of other radicals (particularly OH). Reaction of ozone with NO_2 produces the NO_3 radical, which, during night time, oxidizes several organic pollutants and forms nitric acid and peroxy radicals among other products.

Secondary Organic Aerosol (SOA) is formed from the oxidation products of certain biogenic and anthropogenic VOCs. SOA has been suggested to contribute to climate change [3, 4], adverse human health effects [5, 6], and a reduction in visibility [7]. Previous researches have estimated approximately 70% of organic aerosols are secondary in nature [8]. Glyoxal is a molecule of emerging importance to the atmospheric chemistry community

because of its role in aerosol formation and utility as an indicator for oxidative chemistry. Its tendency to partition to aqueous aerosols is much greater than predicted from it's Henry's law constant due to oligomer formation [9-14]. Corrigan et al. [15] observed reactive uptake of glyoxal onto organic and inorganic aerosol over a wide range of relative humidity (<5 to 50% RH). However, the relative importance of glyoxal in aromatic SOA system is still not well understood.

In addition, organic nitrates are formed in the atmospheric reactions between organic peroxy radicals and NO and between VOCs and NO_3. The specific structure of the R group can be indicative of the nature and origin of the VOC precursor. Peroxyacetyl nitrate (PAN), the most abundant organic nitrates, is derived from both anthropogenic and biogenic VOCs.

Large environmental chambers have seen increased use within the last few years to gather information about the atmosphere in a controlled environment. Some of the key studies of interest have been on secondary organic aerosol (SOA) formation and the evaluation of chemical mechanisms and using the data to develop atmospheric models. The use of large environmental chambers minimizes surface losses along the walls of the chamber. At the University of California Riverside, the Bourns College of Engineering Center for Environmental Research and Technology (CE-CERT) has developed a facility equipped with two 90 m^3 collapsible FEP Teflon reactors on a pressure controlled moveable framework [16]. Arc lamps and black lamps are used to simulate incident solar radiation and a multitude of instrumentation is used to sample from the chamber and collect data. Addition of detectors capable of measuring trace gas concentration provides critical data necessary for model development.

Measurements of trace gas pollutants for smog chamber study or ambient measurement require the use of instrumentation capable of measuring the pollutants at levels as low as parts per trillion (ppt) to several parts per billion (ppb) to elucidate the key atmospheric chemical processes. Trace levels of volatile organic VOC are commonly measured using gas chromatography (GC) and gas chromatography/mass spectrometry (GC/MS)[17]. In addition to organics, many important gases of atmospheric interest (O_3, NO_2, NO_3) possess strong absorption cross sections in the ultraviolet (UV) and visible region. As a result, spectroscopic methods have been developed to measure atmospheric pollutants in real time and continue to be the most commonly used and most reliable techniques for atmospheric measurements. Absorption spectroscopy is an ideal method to employ because of the large absorption cross sections of pollutants in the UV-visible region and the simplicity of the technique. Long path absorption methods such as differential absorption spectroscopy (DOAS) have measured nitrogen dioxide (NO_2), nitrate radical (NO_3), nitrous acid (HONO), and sulfur dioxide (SO_2)[18]. Recently, new spectroscopic methods based on absorption spectroscopy, cavity ring-down spectroscopy (CRDS)[19-21] and cavity enhanced absorption (CEAS)[22], have been implemented for the measurement of pollutants in the atmosphere and smog chamber study.

In this thesis I will be discussing the application of cavity enhanced absorption spectroscopy (CEAS) for measurements of NO_3, NO_2 and glyoxal in smog chamber experiments to study the process of formation of SOA. This thesis provides an experimental dataset to improve model performance by evaluating the model with direct experiments of intermediate products. Product analysis from CEAS measurement is

integrated with other technique and bulk measurements such as particle volume, density, volatility, or elemental ratios.

Reference:

1. Finlayson-Pitts, B.J. and J.N. Pitts, *Chemistry of the upper and lower atmosphere : theory, experiments, and applications*. 2000, San Diego, Calif.: Academic Press. xxii, 969 p.

2. Finlayson-Pitts, B.J. and J.N. Pitts, *Chemistry of The Upper and Lower Atmosphere*. 2000: Academic Press.

3. IPCC. 2007, Intergovernmental Panel on Climate Change (IPCC).

4. Kanakidou, M., et al., *Organic aerosol and global climate modelling: a review.* Atmospheric Chemistry and Physics, 2005. **5**: p. 1053-1123.

5. Davidson, C.I., R.F. Phalen, and S. Solomon, *Airborne particulate matter and human health: A review.* Aerosol Science and Technology, 2005. **39**: p. 737-749.

6. Pope, C.A. and D.W. Dockery, *Health effects of fine particulate air pollution: Lines that connect.* J. Air & Waste Manage. Assoc., 2006. **56**: p. 709-742.

7. Eldering, A. and G.R. Cass, *Source-oriented model for air pollutant effects on visibility.* Journal of Geophysical Research, 1996. **101**(D14): p. 19343-19369.

8. Hallquist, M., et al., *The formation, properties and impact of secondary organic aerosol: current and emerging issues.* Atmospheric Chemistry and Physics, 2009. **9**: p. 5155-5236.

9. Kroll, J.H., et al., *Chamber studies of secondary organic aerosol growth by reactive uptake of simple carbonyl compounds.* Journal of Geophysical Research, 2005. **110**(D23207).

10. Liggio, J., S.-M. Li, and R. McLaren, *Reactive uptake of glyoxal by particulate matter.* Journal of Geophysical Research, 2005. **110**(D10304).

11. Liggio, J., S.-M. Li, and R. Mclaren, *Heterogeneous reactions of glyoxal on particulate matter: identification of acetals and sulfate esters.* Environmental Science & Technology, 2005. **39**: p. 1532-1541.

12. Volkamer, R., et al., *A missing sink for gas-phase glyoxal in Mexico city: Formation of secondary organic aerosol.* Geophysical Research Letters, 2007. **34**(L19807).

13. Volkamer, R., P.J. Ziemann, and L.T. Molina, *Secondary organic aerosol formation from acetylene (C2H2): seed effect on SOA yields due to organic photochemistry in the aerosol aqueous phase.* Atmospheric Chemistry and Physics, 2009. **9**: p. 1907-1928.

14. Galloway, M.M., et al., *Glyoxal uptake on ammonium sulphate seed aerosol: reaction products and reversibility of uptake under dark and irradiated conditions.* Atmospheric Chemistry and Physics, 2009. **9**: p. 3331-3345.

15. Corrigan, A.L., S.W. Hanley, and D.O. De Haan, *Uptake of glyoxal by organic and inorganic aerosol.* Environmental Science & Technology, 2009.

16. Carter, W.P.L., et al., *A new environmental chamber for evaluation of gas-phase chemical mechanisms and secondary aerosol formation.* Atmospheric Environment, 2005. **39**(40): p. 7768-7788.

17. Sipin, M.F., S.A. Guazzotti, and K.A. Prather, *Recent advances and some remaining challenges in analytical chemistry of the atmosphere.* Anal. Chem., 2003. **75**: p. 2929-2940.

18. Sigrist, M.W., *Air monitoring by spectroscopic techniques*. Chemical Analysis. 1994, New York: Wiley.

19. Berden, G. and R. Engeln, *Cavity ring-down spectroscopy: techniques and applications*. 2009: Wiley.

20. Hargrove, J., et al., *Cavity ring-down spectroscopy of ambient NO_2 with quantification and elimination of interferences.* Environ. Sci. Technol., 2006. **40**(24): p. 7868-7873.

21. Brown, S.S., *Absorption spectroscopy in high-finesse cavities for atmospheric studies* Chem. Rev., 2003. **103**(12): p. 5219-5239.

22. Langridge, J.M., et al., *A broadband absorption spectrometer using light emitting diodes for ultrasensitive, in situ trace gas detection.* Rev. Sci. Instrum, 2008. **79**(12): p. 14.

Chapter 2 Instrument

2.1 UCR/ CE-CERT Environmental Chamber

Some studies were conducted in the CE-CERT indoor smog chamber shown in Figure 2- 1 [1], which consists of two, 90m^3 FEP Teflon film reactors suspended by a rigid steel framework within a temperature-controlled enclosure (temperature range 5-45 ℃, normally set to 27 ℃ for experiments). The enclosure is continuously flushed with purified air (Aadco 737 series air purification system). The rigid framework is slowly lowered during the experiments by an elevator to maintain a positive 0.03" H_2O differential pressure between the interior of the reactor and the enclosure. This prevents infiltration of hydrocarbon and other gas-phase compunds through the film wall. A 200 kW argon arc lamp and two banks of 115 W Sylvania black lights are available for simulating solar irradiation within the reactor.

Compounds of interest are introduced to the chamber by passing a stream of pure N_2 over a known volume liquid contained in a glass injection manifold or by flushing pure N_2 through a calibrated glass bulb filled with the gaseous compound to the desired partial pressure. Ozone is made using two Dalton ozone generators (Model Type: OZG-UV-01) and injected the same way with pure N_2 flushing. Relative humidity (RH) inside the chamber can be varied with Controlled Electromantle (EM) Mantle. The lowest RH is normally below 0.1% RH.

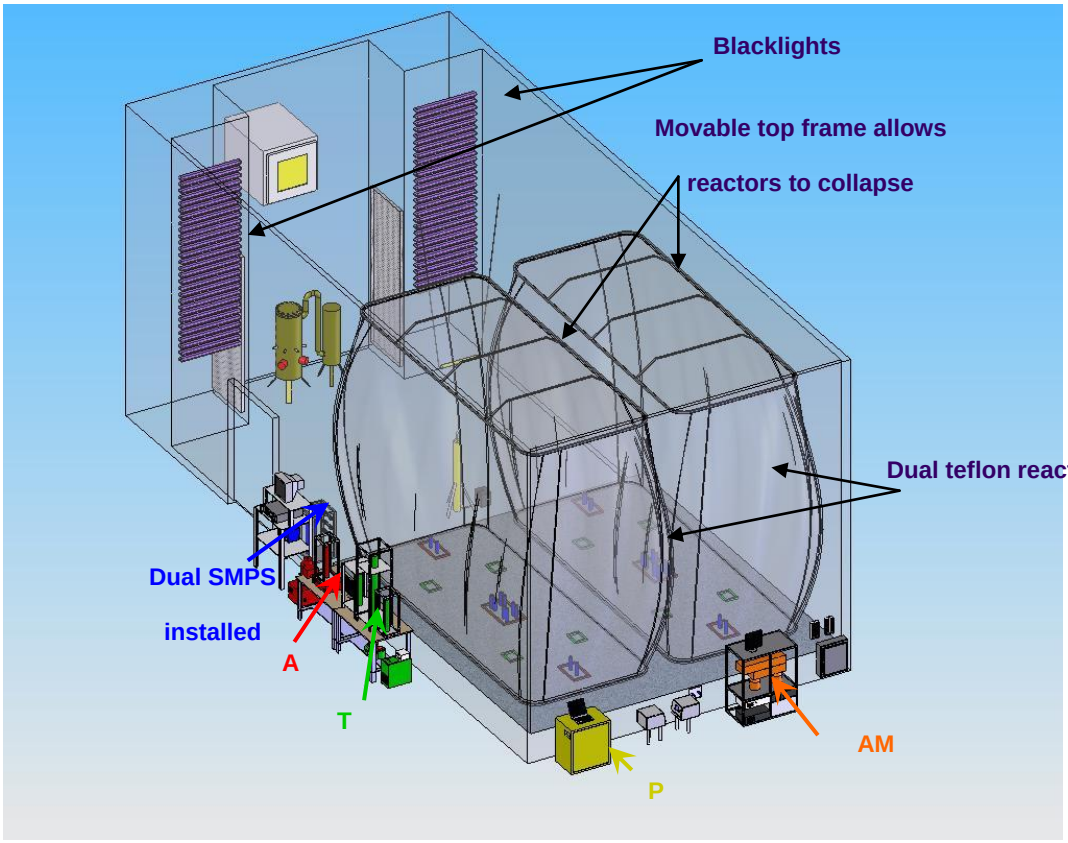

Figure 2- 1. Schematic diagram of CE-CERT chamber facility

2.2 CE-CERT mezzanine chamber

The CE-CERT mezzanine chamber consists of a 12 m^3 volume 2 mil (54 μm) FEP Teflon® film reactor installed in a 2.5 m x 3 m x 7.8 m enclosure, which is shown in Figure 2- 2 . The enclosure is covered with reflective aluminum sheeting and illuminated with 170 of 40W blacklights with peak intensity at 350 nm (SYLVANIA, 350 BL). Six fans are installed underneath to mix the air inside the enclosure with room air to minimize heating in the enclosure. Also there is a minimum of 1 m space between the reactor

surface and blacklights even when the bag is full, thus can avoid overheating of the reactor. Before every experiment, the bag is flushed several times with purified air until the back ground particle concentration is below detection (<0.2 cm^{-3}).

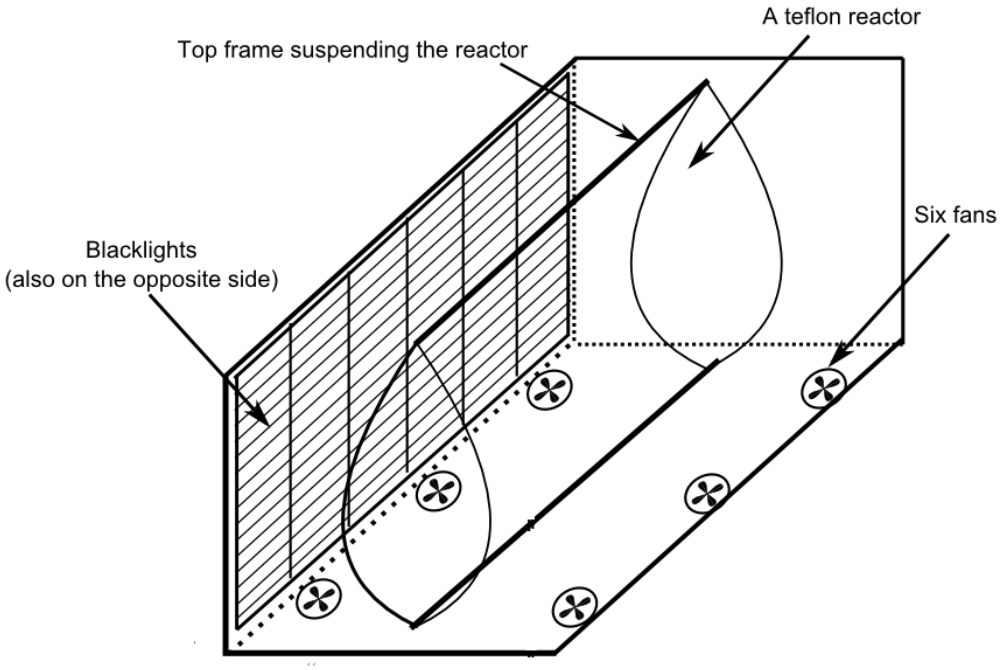

Figure 2- 2. Schematic diagram of CE-CERT mezzanine chamber facility

2.3 Broad-band Cavity Enhanced Absorption Spectroscopy (CEAS)

Cavity enhanced absorption spectroscopy stemmed from cavity enhanced absorption, where a continuous wave incoherent light is injected into a cavity, where the intensity reaches its limiting value and absorption spectra are obtained[2]. The intensity is allowed to build up within the cavity and the absorption coefficient can be derived and the following equation is obtained[3].

$$\alpha(\lambda) = \frac{1}{d}\left(\frac{I_0(\lambda)}{I(\lambda)} - 1\right)(1 - R(\lambda)) \qquad (2.1)$$

where α is the absorption coefficient, d is the length of the cavity, I_0 is the intensity of light exiting the cavity without any absorber present, I is the light intensity of the cavity with absorber, and R is the reflectivity of the mirrors. It should be noted that all variables with the exception of the length of the cavity are wavelength dependent. The resolution of this technique is dictated by the slit width and grating of the monochromator. The sensitivity is dependent on the mirror reflectivity, which should be characterized to provide the correct absorption coefficient. To obtain absolute concentration information of absorbers the mirror reflectivity must be known[4]. Typical mirror reflectivities used range from R=0.999 to R=0.9999. Independent measurements of mirror reflectivity can be measured a few ways. One way is by using a calibration gas that is known to absorb in the region of interest such as NO_2 with a known concentration and extracting mirror reflectivity information by fitting the spectrum obtained with the literature spectrum of NO_2[5]. Another method used to obtain mirror reflectivity data is using the CRDS technique and measuring the reflectivity offline[6]. The mirror reflectivity is extracted from the wavelength dependent ring down time. The CRDS method of obtaining mirror reflectivity data typically yields higher reflectivity values because there are fewer losses of light within the cavity when a pulsed laser is used as opposed to the uncollimated light from an LED or xenon arc lamp. In this case, we calibrate our mirror reflectivity with known concentration of NO_2.The transmission signal without any absorbers present, I_0, must also be measured prior to measurements with an absorber present in the cell. Therefore, the fluctuating background from the

source can affect the sensitivity and it is important to maintain a stable source to minimize error from the fluctuation especially during long periods of sampling. This is achieved by mounting the light source to a Peltier cooler or thermo electric cooler (TEC) and a heat sink with a fan to provide additional cooling.

CEAS provides the long optical path that absorption spectroscopy can benefit from to improve sensitivity. It also has the advantage of not requiring an expensive light source that is typically required for pulsed CRDS[7]. The use of a high powered LED or xenon arc lamp is sufficient[8]. CEAS has the potential for simultaneous analysis of multiple absorbers in the same spectral regionThe typical setup of a CEAS instrument is shown in Figure 4.1. The incoherent light source can either be from a xenon arc lamp using a filter for wavelength selection or a high powered LED with a broad emission of a few tens of nanometers[5]. A filter may or may not be needed depending on the LED. The light is coupled into the cavity using a lens to focus and couple the light into the spectrometer. The length of the cell can vary from lengths of less than a meter to lengths of a few meters. Longer cell lengths offer longer effective pathlengths. As the light exits the cavity, it is refocused using a lens. The focused light is imaged onto fiber optics that steer the light into a monochromater, where it is then detected using a CCD.

CEAS is a simple absorption spectroscopy method using inexpensive LEDs as the light source and has the potential for measuring multiple absorbers simultaneously. In this thesis, two instruments based on CEAS are developed. One uses a red LED and measure NO_3 in the 662 nm region and is applied to the detection of the nitrate radical in an environmental chamber. The second device uses a high powered LED in the 450nm region and is developed for measurements of NO_2 and glyoxal simultaneously for

environmental chamber study. All of the NO_3, NO_2 and glyoxal experiments investigated in this thesis utilize these two CEAS.

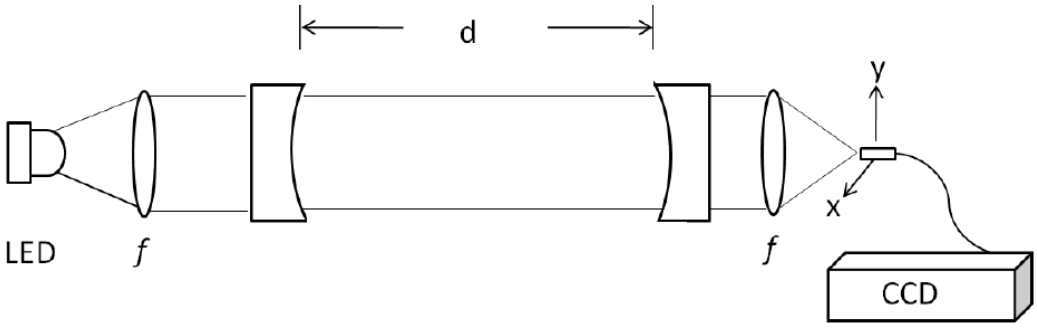

Figure 2- 3. Typical CEAS arrangement. The light source used can either be a xenon arc lamp or an LED. A focusing lens is used to collimate the light and inject it into the cell composed of two high reflective mirrors (R>0.99). The high reflective mirrors are separated by a distance, d. The light exiting the cavity is focused using a focusing lens onto an x-y translational fiber optic cable leading to the CCD.

Reference:

1. Carter, W.P.L., et al., *A new environmental chamber for evaluation of gas-phase chemical mechanisms and secondary aerosol formation.* Atmospheric Environment, 2005. **39**(40): p. 7768-7788.

2. Engeln, R., et al., *Cavity enhanced absorption and cavity enhanced magnetic rotation spectroscopy.* Review of Scientific Instruments, 1998. **69**(11): p. 3763-3769.

3. Fiedler, S.E., A. Hese, and A.A. Ruth, *Incoherent broad-band cavity-enhanced absorption spectroscopy of liquids.* Review of Scientific Instruments, 2005. **76**(2): p. 023107-023107-7.

4. Venables, D.S., et al., *High sensitivity in situ monitoring of NO_3 in an atmospheric simulation chamber using incoherent broadband cavity-enhanced absorption spectroscopy.* Environmental Science & Technology, 2006. **40**(21): p. 6758-6763.

5. Schuster, G., I. Labazan, and J.N. Crowley, *A cavity ring down/cavity enhanced absorption device for measurement of ambient NO_3 and N_2O_5.* Atmospheric Measurement Techniques, 2009. **2**(1): p. 1-13.

6. Ball, S.M., J.M. Langridge, and R.L. Jones, *Broadband cavity enhanced absorption spectroscopy using light emitting diodes.* Chemical Physics Letters, 2004. **398**(1-3): p. 68-74.

7. Ayers, J.D., et al., *Off-axis cavity ringdown spectroscopy: application to atmospheric nitrate radical detection.* Applied Optics, 2005. **44**(33): p. 7239-7242.

8. Triki, M., et al., *Cavity-enhanced absorption spectroscopy with a red LED source for NOx trace analysis.* Applied Physics B-Lasers and Optics, 2008. **91**(1): p. 195-201.

Chapter 3. Chamber study of Nitrate Radical (NO_3) by Cavity Enhanced Absorption Spectroscopy (CEAS)

3.1 Introduction

The nitrate radical (NO_3) plays a large role in the nitrogen oxide (NO_x) chemistry in the atmosphere[1]. During the daytime, the main oxidant in the atmosphere is the hydroxyl radical (OH). However, at night when OH radical concentrations are low, NO_3 is considered to be the major oxidation species often reacting with biogenic volatile organic hydrocarbons (VOCs) emitted during the nighttime air. The primary source for NO_3 is the reaction of nitrogen dioxide, NO_2, with ozone; once the sun has set stopping NO_3 photolysis, concentrations rise throughout the night. The typical concentrations of NO_3 range from 10's of parts per trillion (ppt) in remote locations to 100's of ppt in more polluted environments[2]. The formation of nitric acid from NO_3 abstraction of a hydrogen atom from a hydrocarbon is considered a sink, which results in the hydrocarbon radicals that subsequently react with oxygen molecules to produce peroxyl radicals (RO_2) [2]. When NO_3 reacts with NO_2 present at night it forms dinitrogen pentaoxide (N_2O_5). The heterogeneous uptake of N_2O_5 on surfaces of particulates such as ammonium sulfate and ammonium bisulfate to form nitric acid has been measured in the troposphere and is another known sink for NO_x in the troposhere [3]. Additionally, the reaction of NO_3 with linear alkenes may contribute to secondary organic aerosol (SOA) formation [4, 5].

Much of the current research of NO_3 has involved its removal from the atmosphere through surface reactions of aerosol and its contribution to aerosol formation. However, measurements of NO_3 in the atmosphere as well as lab measurements have been limited[6]. Thus, instrumentation that is inexpensive, portable, as well as sensitive is needed to measure NO_3 to gain better insights into its removal pathways in the atmosphere. Cavity Enhanced Absorption Spectroscopy (CEAS) is a sensitive and portable method for the measurement of NO_3[7]. It has the advantage of a long effective absorption path length in a compact setup, and sensitivity (ppt level) and the use of an inexpensive light emitting diode as a broadband light source allows for the simultaneous analysis of multiple absorbers. Instrumentation that can provide insights into the reactions and variability of the nitrate radical during the nighttime atmosphere can shed light on sinks, which are valuable to computer models that provide information on atmospheric pollutants and their sources and sinks.

The trend of instrumentation for NO_3 detection has been towards portable and robust analyzers. Here a sensitive and portable instrument based on Cavity Enhanced Absorption Spectroscopy (CEAS) has been developed for the measurement of NO_3[8]. A detailed introduction to the CEAS technique is introduced in Chapter 2. Briefly, the absorption coefficient of the sample can be determined from the measurement of continuous light transmitted into a cavity composed of high reflective mirrors using the equation:

$$\alpha(\lambda) = \frac{1}{d}\left(\frac{I_0(\lambda)}{I(\lambda)} - 1\right)(1 - R(\lambda)) \qquad (3.1)$$

Where I is the transmission of light with an absorbing medium present and Io is the transmission without an absorber, R is the reflectivity and, d is the length of the cavity.

CEAS has the advantage of a long effective absorption pathlength in a compact setup (~1m), and sensitivity (ppt level) and the use of an inexpensive light emitting diode as a broadband light source and a CCD detector allows for the simultaneous analysis of multiple absorbers.

In this chapter, CEAS has been presented as an inexpensive portable NO_3 analyzer to conducts measurements in an environmental chamber to study the NO_3 reactions and provide data for atmospheric models.

3.2 Experimental

The typical setup of a CEAS instrument is shown in Figure 2.1. The incoherent light source is from a high powered LED with a broad emission of a few tens of nanometers. The light is coupled into the cavity using a lens to focus and couple the light into the spectrometer. The length of the cell can vary from lengths of less than a meter to lengths of a few meters. The glass cell described here is approximately 65 cm long, 2.54 inches in diameter, with a wall thickness of 1/16 inches. Three inlet tubes (3/8 inch diameter, 1/16 inch thick) are constructed along the glass cell, which are used as an inlet port, an outlet port and as a port used to connect a pressure gauge (Cole Parmer). As the light exits the cavity, it is refocused using a lens. The focused light is imaged onto fiber optics that steer the light into a monochromater, where it is then detected using a CCD. The instrument is used under ambient condition, in which the pressure is about 715-735 torr with the flowrate of sample gas is 8L/min at room temperature.

In the setup, the CCD collects transmission spectra using an exposure time of 0.5 seconds with 240 samples accumulated for an overall sampling time of 2 minutes. An exposure time of 0.5 seconds was chosen to prevent saturation of the signal at the peak LED emission spectrum at a maximum operating power of 500 mW. The background signal under the same acquisition conditions is collected with the LED off and the background is subtracted from the transmission spectra.

3.3 Data Analysis

Data was acquired using the software provided by the Andor CCD detector. Data was then saved in ASCII file format for analysis offline using a custom program written in the laboratory using the Labview software. Spectra are obtained through processing using the CEAS equation, which requires the transmission spectra without, I_o, and with, I, absorber and the mirror reflectivity at the 662 nm region. The spectral region containing the strong absorption feature of NO_3 at 662 nm is fitted using the NO_3 cross section from 655 nm to 675 nm. In addition to NO_3, the absorption features of NO_2 and water are also included in the fit and the number density or concentration is extracted for NO_3. It should be mentioned that the chamber experiments are typically carried out without any humidity. The unknown parameters are extracted using a linear algebraic method known as the singular value decomposition (SVD) method. The equation for the nonlinear polynomial fit is shown below:

$$a(\lambda) = b_0 + b_1\lambda + b_2\lambda^2 + n_{H_2O}\sigma_{H_2O}(\lambda) + n_{NO_3}\sigma_{NO_3}(\lambda) + n_{NO_2}\sigma_{NO_2}(\lambda) \qquad (3.2)$$

Where, a (λ), is the wavelength dependent absorption coefficient, σ, is the cross section of the absorbing molecule and, n, is the number density of each absorber. The background signal is represented by b_0, $b_1\lambda$, and $b_2\lambda^2$. The best spectral fit will have minimized the residuals from the experimental data. The output data provides number density information for the absorbers in the spectral region of interest, typically a few nanometers (~10 nm) in the 662 nm region. For this instrument, the lowest detectable signal for the instrument is approximately 10 ppt per 2 minutes of integration time.

3.4 NO_3 Characterization Chamber study

To characterize the response of the CEAS detector, two chamber experiments for NO_3 were carried out. The first one is shown in Figure 3- 1, in this experiment, NO_3 was generated from the reaction of NO_2 and ozone inside a dark environmental chamber at CE-CERT. In the chamber, the reaction levels out at a concentration of around 4 ppb. N_2O_5 was then introduced into the environmental chamber producing NO_3 from thermal decomposition and a subsequent rise in signal is observed at around 200 minutes. The signal decreases over time signifying the radical is terminated from wall collisions or production of NO_2 from any ozone remaining in the chamber from the reaction used to generate the nitrate radical initially. Excess isoprene is then introduced into the chamber at around 310 minutes of the experiment and the NO_3 remaining becomes oxidized. Isoprene was selected for the model/demonstration as it is an important and relevant reaction observed in the atmosphere [4, 9]. After the injection of isoprene, the NO_3 concentration level dropped rapidly and reached zero in ~ 15 min.

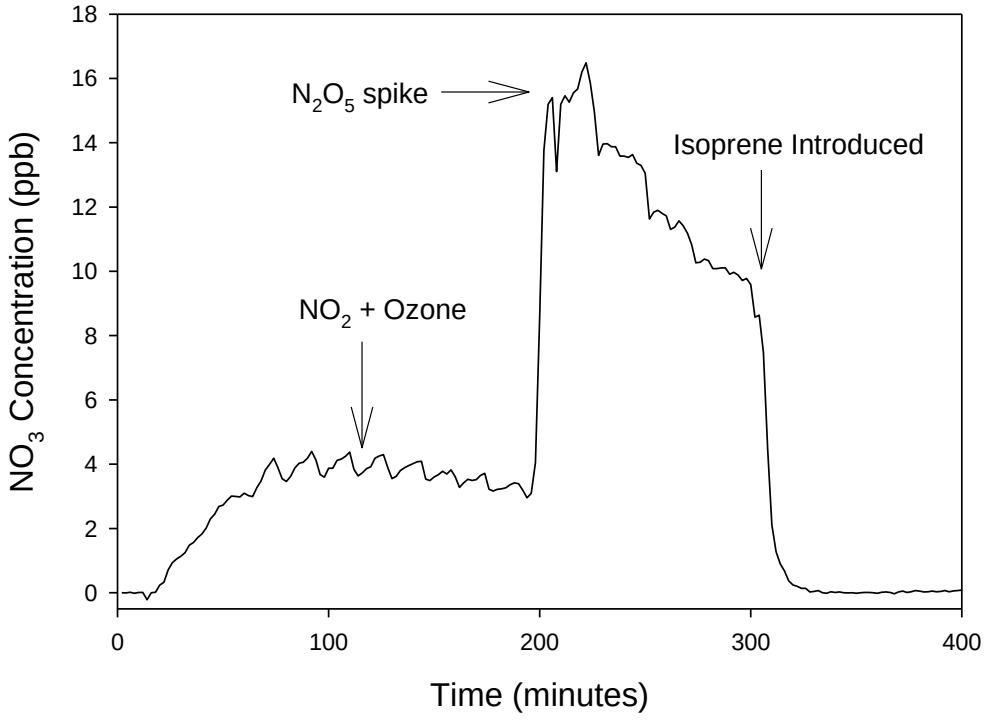

Figure 3- 1. NO_3 measurement conducted at CE-CERT chamber.

A second chamber characterization experiment for NO_3 is carried out for NO_3 wall loss under dry and humid condition, which is shown in Figure 3-2. In this experiment, N_2O_5 was injected into the chamber as a NO_3 source at 50min. From 50min to 130min the NO_3 level decreased from its maximum ~160ppt to only ~3ppt, which is because of wall loss of NO_3 or N_2O_5 in the chamber. At 130 min, humid air was injected into the chamber which caused the NO_3 concentration dramatically droped to 0 ppt in about 10min. This may due to either the wall loss of NO_3 radical in the humid air or the wall loss of N_2O_5 in the humid air or both, which requires further investigation. This experiment characterized the NO_3 behavior in the chamber which provides valuable information for chamber experiments of NO_3.

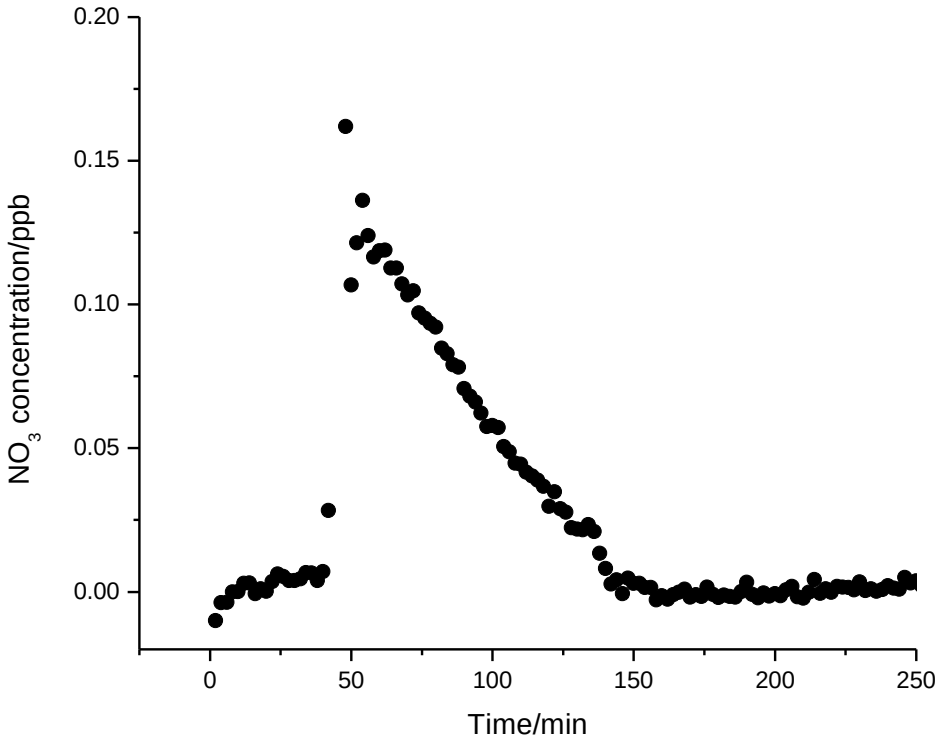

Figure 3- 2. Chamber experiment for detecting NO_3 wall loss under dry and humid condition. Humid air was added at 130min.

3.5 NO_3 and amine kinetics chamber study

Amines are known to be emitted from natural and anthropogenic sources. Numerous studies have shown that significant concentrations of amines are present near agricultural facilities such as dairies, feedlots, and other animal feeding operations (AFOs)[10]. Butylamine (BA) and diethylamine (DEA) are reported as the most important amines emitted from a Northern California dairy[11]. Trimethylamine (TMA) has been indicated as an important VOC in a number of studies. Very little work has focused on the atmospheric chemistry or the secondary organic aerosol formation from amines[12]. There is currently no literature data exists on the nitrate radical reactivity of these amine compounds while nitrate radical may play a significant role in amine oxidation at night

Another experiment that is ongoing at CE-CERT involves the reaction of NO_3 with amines to quantify the SOA formation potentials of TMA, DEA and BA under different conditions. Using the NO_3 CEAS, the absolute gas-phase reaction rate between the amines and NO_3 can be obtained. In addition, a well studied and characterized relative rate method is carried out to determine the gas-phase reaction rate between the amines and NO_3. This method uses a two component reaction system with one component having known, similar reaction kinetics to the molecule of interest. The relative reaction rate between the known chemical and the oxidant (in this case nitrate), coupled with the decay rate of the gaseous compound of interest (amines), is then used to accurately assess the reaction rate.

One reaction of interest involves NO_3 and DEA. The typical reaction profile of NO with DEA is shown in Figure 3- 3. DEA is introduced into the chamber followed by

introduction of N_2O_5. Over the span of the 12 hour experiment the NO_3 signal decreases from a peak of ~ 1 ppb until the reaction undergoes completion by following the reaction profile.

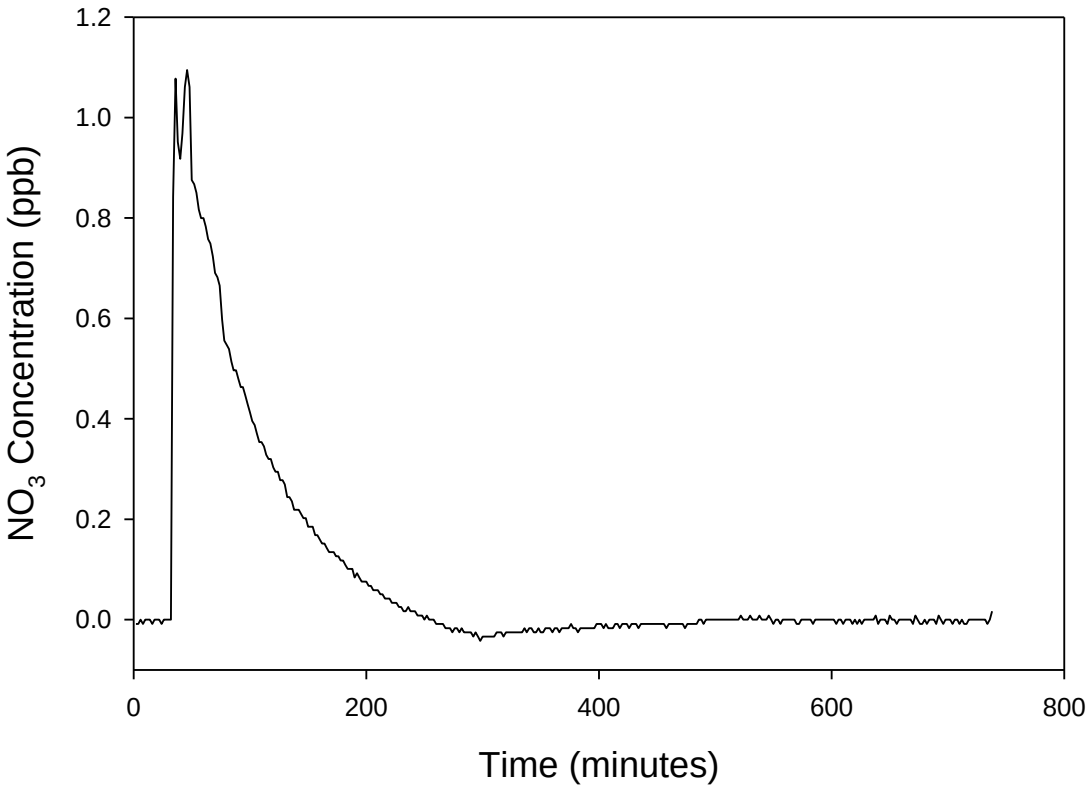

Figure 3- 3 NO_3 measurement conducted at CE CERT chamber. Signal disappears due to reaction with DEA.

3.6 Conclusion

A sensitive and portable CEAS NO_3 detector having a 10 ppt / 2min has been developed and used in smog chamber study. A detailed description of the construction and development of the NO_3 instrument based on CEAS is given. The sensitivity is

expected to improve with higher reflectivity mirrors. Environmental chamber measurements of NO_3 with isoprene and diethyl amine are performed to demonstrate the instrument's capability. The reaction of NO_3 with amines continues to be an ongoing project at the CE-CERT environmental chamber. This preliminary data demonstrate the capability of kinetics study of reactions between amine and NO_3.

References

1. Platt, U., et al., Detection of NO_3 in the polluted troposphere by differential optical-absorption. Geophysical Research Letters, 1980. **7**(1): p. 89-92.

2. Finlayson-Pitts, B.J. and J.N. Pitts, Chemistry of the Upper and Lower Atmosphere. 2000: Academic Press.

3. Brown, S.S., et al., Variability in nocturnal nitrogen oxide processing and its role in regional air quality. Science, 2006. **311**(5757): p. 67-70.

4. Fry, J.L., et al., Organic nitrate and secondary organic aerosol yield from NO_3 oxidation of beta-pinene evaluated using a gas-phase kinetics/aerosol partitioning model. Atmospheric Chemistry and Physics, 2009. **9**(4): p. 1431-1449.

5. Rollins, A.W., et al., Isoprene oxidation by nitrate radical: alkyl nitrate and secondary organic aerosol yields. Atmospheric Chemistry and Physics, 2009. **9**(18): p. 6685-6703.

6. Brown, S.S., H. Stark, and A.R. Ravishankara, Cavity ring-down spectroscopy for atmospheric trace gas detection: application to the nitrate radical (NO_3). Applied Physics B-Lasers and Optics, 2002. **75**(2-3): p. 173-182.

7. Schuster, G., I. Labazan, and J.N. Crowley, *A cavity ring down/cavity enhanced absorption device for measurement of ambient NO_3 and N_2O_5.* Atmospheric Measurement Techniques, 2009. **2**(1): p. 1-13.

8. Venables, D.S., et al., *High sensitivity in situ monitoring of NO_3 in an atmospheric simulation chamber using incoherent broadband cavity-enhanced absorption spectroscopy.* Environmental Science & Technology, 2006. **40**(21): p. 6758-6763.

9. Perring, A.E., et al., *A product study of the isoprene+NO_3 reaction.* Atmospheric Chemistry and Physics, 2009. **9**(14): p. 4945-4956.

10. Ge, X., A.S. Wexler, and S.L. Clegg, *Atmospheric amines - Part I. A review.* Atmospheric Environment, 2011. **45**(3): p. 524-546.

11. Rabaud, N.E., et al., *Characterization and quantification of odorous and non-odorous volatile organic compounds near a commercial dairy in California.* Atmospheric Environment, 2003. **37**(7): p. 933-940.

12. Erupe, M.E., et al., *Secondary organic aerosol formation from reaction of tertiary amines with nitrate radical.* Atmos. Chem. Phys. Discuss., 2008. **8**(4): p. 16585-16608.

Chapter 4 Cavity enhance absorption spectroscopy for Evaluating NO_x Sinks and Recycling in Environmental Chamber study

4.1 Introduction.

Atmospheric chemical reactions involving volatile organic compounds (VOCs) and NO_x results ozone formation; deep understanding of chemical mechanism of atmospheric ozone formation is needed. Most VOCs react to remove NO_x by forming NO_x sink compounds such as organic nitrates, peroxy nitrates, or nitro compounds, which consequently reduces O_3 level. Some VOCs, like aromatics, are strong NO_x sinks such that increasing their emissions results can reduce O_3 under NO_x-limited conditions. However, most of these NO_x sink VOCs may eventually react to return NO_x back to the atmosphere (NO_x recycling) ultimately causing additional downstream O_3 production in NO_x-limited regions.

Therefore, it is very important to understand the NO_x sinks and NO_x recycling chemical mechanisms to predict effects of VOC and NO_x controls on ozone formation. However, the chemical mechanisms have uncertainties, and their predictive capabilities need to be evaluated by comparing their predictions against results of environmental chamber experiments[1]. Most of the currently available chamber experiments were designed to test the rate at which different VOCs promote ozone formation in the presence of NO_x. Although

such experiments can have some sensitivity to NO_x-sink processes, they are not adequate to fully evaluate model predictions of NO_x sinks or sources generated from atmospheric oxidation of VOCs.

Therefore, a new project was necessary whose objective was to design and carry out environmental chamber experiments to test model predictions of effects of NO_x sinks and sources in VOC atmospheric reactions and to provide information for improving atmospheric mechanisms.

In this project, the specific VOCs studied included the aromatic hydrocarbon toluene, the aromatic NO_x removing product o-cresol, the potentially NO_x releasing product 2-nitrophenol, and furan, which reacts to form 2-butene - 1,4-dial, a representative photoreactive aromatic ring-opening product[2], in near-100% yields[3, 4]. In addition, experiments with representative organic nitrates, isopropyl nitrate and isobutyl nitrate, were studied to evaluate NO_x recycling from reactions of organic nitrates formed from alkanes and other compounds. Finally, NO_x sink and single compound experiments with isoprene were also included because this biogenic compound dominates regional emissions in many NO_x-limited areas and also may also have significant NO_x sink processes.

In my thesis work, I focus on an important portion of this project, which is to develop a CEAS instrument for measuring NO_2 concentration for these chamber experiments and process the data analysis to evaluate the NO_2 concentration. The CEAS system for measuring NO_2 was newly installed for this project. It provides the most reliable and interference-free method for monitoring NO_2. By using CEAS for NO_2, preliminary data is obtained and integrated with other technique in this study, and we also teamed up with our

modeling members. Under this condition, the presence of NO_x recycling processes in the reactions of those VOCs is confirmed and further modeling study will be discussed.

4.2 Experimental

4.2.1 Cavity enhanced absorption spectroscopy NO_2 method.

Cavity enhanced absorption spectroscopy (CEAS) was used to measure NO_2 for most of the experiments for this project, which has been described in Chapter 2. CEAS provides a relatively long optical path and sensitively measures the transmitted light intensity through an optical cavity bounded by two (or more) high reflectivity mirrors[5-9]. CEAS also has the advantage of not requiring an expensive light source that is typically required for pulsed cavity ring-down spectroscopy (CRDS). A high powered light-emitting diode (LED) or xenon arc lamp is sufficient as a light source for CEAS[7, 8]. CEAS has the potential for simultaneous analysis of multiple absorbers in the same spectral region (e.g., both NO_2 and glyoxal in the 440 – 460 nm region[9]). For this project, incoherent continuous-wave broadband CEAS was used to measure NO_2, and this type of CEAS was previously used to measure NO_2 by Langridge et al.[8]. The major components of this CEAS system include a glass cell housing the optical cavity (65 cm long, 2.54 cm diameter with 1/16 inch wall thickness), two high reflectivity mirrors, three inlet tubes (3/8 inch diameter, 1/16 inch thickness) for one sample inlet port, one outlet port and one port for connecting a pressure gauge (Cole Parmer), an LED (Luxeon) as the light source, and a charge-coupled device (CCD) as the light detector, a lens to focus and couple the light originating from the LED

into the optical cavity, a lens to refocus the cavity output light that is imaged onto fiber optics steering the light into a monochromater where the light is then detected using the CCD. During this project, the pressure inside the optical cavity was 714~720 torr (0.939-0.947 atm), and the flow rate of sample gas was 1 liter/minute. In the setting used, the CCD collects transmission spectra using an exposure time of 0.5 second with 112 samples accumulated during an overall sampling time of 1 minute. The exposure time, 0.5 second, was chosen to prevent the saturation of the signal at the peak LED emission spectrum at the maximum operating power of 200 mW for this CEAS system. The background signal under the same acquisition conditions was collected with the LED off and the background was subtracted from the transmission spectra.

The light absorption coefficient (α) can be obtained by using CEAS-measured light intensities with and without the light absorbing gases (I and I_o, respectively), wavelength-dependent mirror reflectivity (R) and the cavity length (d) as follows in eqn (2.1)

For this project, the mirror reflectivity required to calculate α was determined to be 0.9998 by running a dark chamber experiment where NO_2 was injected multiple times to establish different levels of NO_2 and by comparing NO_2 measurements by the NO_x analyzer. Then, the number concentration of the light absorber *i* (n_i in molecules/cm^3) can be calculated by using a relationship between the absorption coefficient and the number concentration,

$$\alpha_i(\lambda) = \sigma_i(\lambda) \cdot n_i \qquad (4.1)$$

where λ is the wavelength and σ is the absorption cross-section of the absorber and by making a best fit typically using a polynomial equation to take care of light extinction by the background molecules (e.g., N_2 and O_2) and other co-existing light absorbing molecules (e.g., glyoxal) in the wavelength range covered by the CEAS instrument as illustrated below by the equation used for this project:

$$\alpha(\lambda) = b_o + b_1 \cdot \lambda + b_2 \cdot \lambda^2 + b_3 \cdot \lambda^3 + \sigma_{NO2}(\lambda) \cdot n_{NO2} + \sigma_{Glyoxal}(\lambda) \cdot n_{Glyoxal} \quad (4.2)$$

Wavelength-dependent absorption cross-sections (σ(λ)) are available in the literature and representative data evaluation web sites (e.g., IUPAC, 2006 and NASA, 2006), and converting number concentrations (in molecules/cm^3) into concentrations in parts per billion (ppb) with a given temperature and pressure can be done using an equation based on the ideal gas law.

$$C(\text{in ppb}) = \frac{(\text{Temperature in K}/298)}{2.463 \times 10^{10} (\text{Pressure in atm})} \times C(\text{in molecules}/\text{cm}^3) \quad (4.3)$$

Data were acquired using the software provided by the CCD detector (Andor; http://www.andor.com), and saved in the ASCII format for offline analysis using a custom program written in Labview. Spectra were obtained using the CEAS fitting equation described above at the 445-455 nm range. This spectral region which contains the strong absorption feature of NO_2 at 448 nm was fitted using the NO_2 cross sections provided by Burrows et al.,[10]. In addition to NO_2, the absorption features of glyoxal were also included in the fitting equation and the interference of glyoxal was corrected. The glyoxal concentration could be obtained in this study and its results will be discussed later in Chapter 5. The unknown parameters were extracted using a linear algebraic method known as the singular value decomposition (SVD) method. The best spectral fit will result in

minimizing the residuals from the experimental data. Figure 4-1 shows an example from snapshot of Labview program of CEAS NO_2 measurement. In this figure the line is the fitting curve for 50ppb NO_2 while dots stand for the data output from the measurement

The output data provide number density information for the absorbers in the spectral region of interest, typically ~10 nm in the 450 nm region. However, occasionally, using the entire region of 10 nm width resulted in artificial negative values because sometimes the 3rd order polynomial fit could not adequately describe the background signal. In those cases, alternately, a smaller wavelength range (446.5 nm to 450.0 nm) was used for fitting the raw data while utilizing only the strongest NO_2 absorption peak.

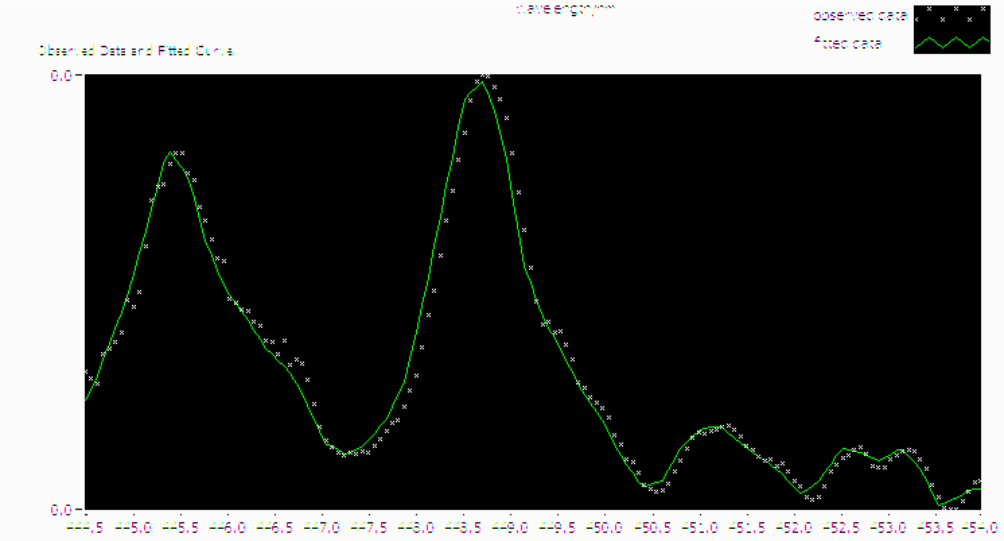

Figure 4- 1 Labview program snap short for 50 ppb NO_2. x axis is the LED wavelength ranging from 444.5nm to 454 nm; y axis is the relative intensity. Line is the fitting curve for 50ppb NO_2 while dots stand for the data output from the measurement

The CEAS system has been fully calibrated using known concentrations of NO_2. When the instrument first installed in our chamber, calibration experiments with known

concentration of NO_2 have been carried out with NO_2 standard tank and zero air. Furthermore, NO_2 concentrations in the chamber are compared with NOx analyzer.

Figure 4-2 shows the good agreement that can be obtained between these two instruments under normal chamber operation. For every experiment, NO_2 concentrations established during sampling from the zero air (purified air) and during gas phase titration (GPT) using reaction between NO and O_3 to generate a specified concentration of NO_2 were used as reference NO_2 concentrations for calibrating the CEAS system during the chamber experiments for everyday calibration[11], Fried and Hodgeson[12], Bertram et al.[13]).

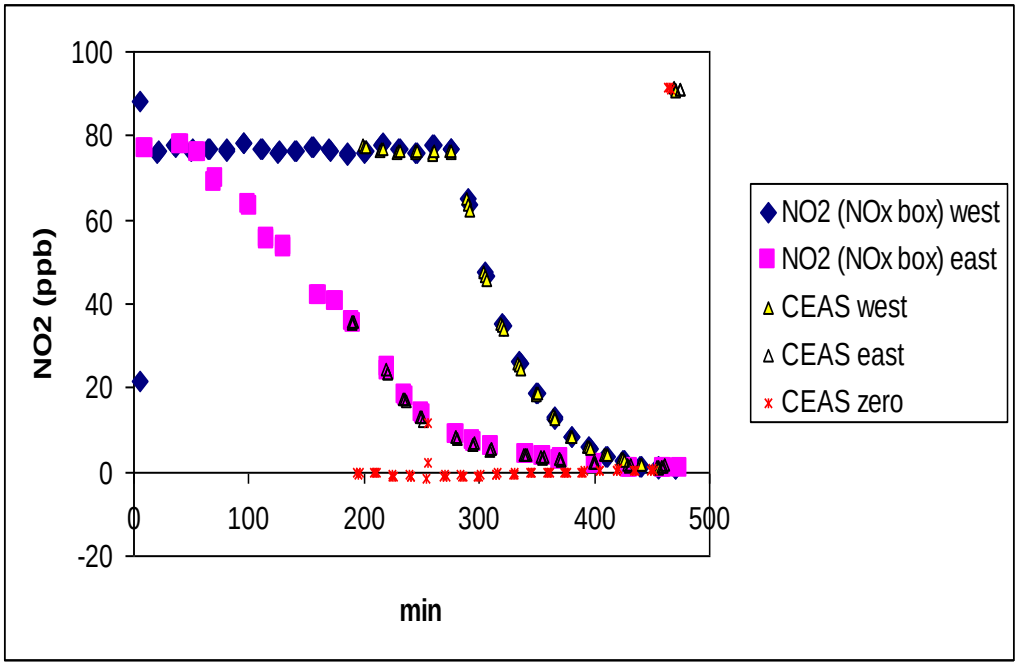

Figure 4- 2 Chamber calibration experiment of NO_2 concentration comparison between CEAS and NOx analyzer

The CEAS analysis suffered from zero drift in many experiments, so this was corrected by cycling between sampling from the reactor and zero air, and interpolating the zero values

for the times of the reactor measurements for the purpose of zeroing these data. In some cases zero values for spans had to be extrapolated.

An attempt was made to use this CEAS system to measure total peroxy acyl nitrates (PANs, or $RC(O)OONO_2$) and total organic nitrates ($RONO_2$) after thermally dissociating those nitrogen compounds using a glass tube surrounded by a heating tape [14] for thermal dissociation). However, the utility of the data obtained in this way during this project for accurately measuring total PANs or organic nitrates was not established, so these data are not considered useful for model evaluation at this time. Therefore, the results of the thermal desorption measurements made during this project are not discussed further here.

4.4.2 Experimental procedure and operation conditions.

Besides CEAS for NO_2 measurement, many other instruments have been used. The environmental chamber has been described in Chapter 2. Table 4-1 gives a listing of the analytical and characterization instrumentation whose data were utilized for this project.

Table 4- 1 List of analytical and characterization instrumentation for the UCR EPA chamber

Type	Model or Description	Species	Sensitivity
Ozone Analyzer	Dasibi Model 1003-AH. UV absorption analysis.	O3	2 ppb
NO - NOy Analyzer	TECO Model 42 C with chemiluminescent analysis for NO, NOy is converted to NO by catalytic conversion.	NO	1 ppb
		NOy	1 ppb
CEAS	In-house cavity enhanced absorption spectroscopy	NO2	~0.5 ppb
GC-Luminol	Fitz Aerometric Technologies Model 008 gas chromatography – luminol system for NO2 and PAN	NO2 PAN	~0.15 ppb
CO Analyzer	Thermo Environmental Instruments Model 48 C	CO	50 ppb
GC-FID Instruments	HP 6890 Series II GCs with dual columns, loop injectors and FID detectors. Controlled by computer interfaced to network.	VOCs	~10 ppbC
GC-FID Instruments with cartridge sampling	Agilent 6890 GC with FID detection interfaced to a ThermoDesorption System (CDS analytical, ACEM9305, Sorbent Tube MX062171) with Tenax-TA/Carbopack/ Carbosieve S111.	Lower volatility VOCs	~1 ppbC
Gas Calibrator	Model 146C Thermo Environmental Dynamic Gas Calibrator	N/A	N/A
Data Acquisition Sytem	Windows PC with custom LabView software, 16 analog input, 40 I/O, 16 thermo-couple, and 8 RS-232 channels.	N/A	N/A
Temperature sensors	Various thermocouples, radiation shielded thermocouple housing	Temperature	~0.1 oC
Scanning Mobility Particle Sizer (SMPS)	TSI 3080L column, TSI 3077 85Kr neutralizer, and TSI 3760A CPC.	Aerosol number and size distributions	Adequate

Detailed experimental procedure and operation conditions are described in the report of Texas Air Quality Research [15]. Briefly speaking, all the experiments for this project were carried out in an indoor environmental chamber with black light as light source. Before each experiment, both reactors were thoroughly flushed with dry purified air and filled to their maximum volume. Common reactants for both reactors were simultaneously injected and then mixed. Once reactant levels have stabilized and samples were taken for analysis to determine initial reactant concentrations, the irradiations were begun by turning on the lights. Sampling was conducted alternatively or simultaneously from both reactors during the irritation. The experiments were ended after about 8 hours or when both reactors were depleted and simultaneous measurements were carried out.

A total of 55 runs in environmental chamber experiments were carried out in the UCR EPA chamber for this project, as summarized below in Table 4-2 . Among them, most of the experiments have usable CEAS NO_2 measurement. In these experiments, different VOCs have been chosen whose results will be discussed in 4.3 section.

Table 4- 2 list of runs in this project and their brief purpose.

Runs	Type
20	NO_x Sink with base case (10 test runs, each with a base case)
4	NO_x sink without base case (test reactant accidentally injected into both reactors)
8	NO_x Source (two methods)
3	Isoprene - NO_x, with varied initial concentrations (one duplicate experiment excluded)
6	Ethene or Propene - NO_x Control (two duplicate experiments excluded)
3	NOx source control (NO_x added)
9	Background NO_x characterization (two methods)
2	Radical source characterization

4.3 Results and discussion.

As an important part of the whole project, this thesis only focuses a portion of the project. Some of the results are analyzed by other instruments and integrated with modeling study.

4.3.1 Results of NO_x Sink Experiments

NO_x sink experiments were carried out for toluene, o-cresol, furan (a precursor to the aromatic fragmentation product 2-butene-1,4-dial), and isoprene, using ethene - NO_x as the base case experiment in all cases, and also using propene - NO_x as the base case for toluene.

Most NO_x sink experiments had data for NO_2 that are useful for modeling, and the NO_2 data from most of the base case experiments were generally consistent with model predictions. The CEAS NO_2 data are judged to be somewhat less subject to interferences and have fewer experimental issues, so are preferred for modeling. Since the purpose of this thesis is not on analysis of the whole data set, an example of the concentration time plots of the data potentially useful for modeling on Figure 4-3 for the toluene runs. In this figure, different symbols are used for the NO_2 data obtained using the CEAS vs. the GC-Luminol instruments, which showed that in some cases the two methods may not be consistent. The figure also includes SAPRC-07 model simulations of the base case experiments, where applicable. Plots for other investigated systems can be found in the report of Texas Air Quality Research Program[15].

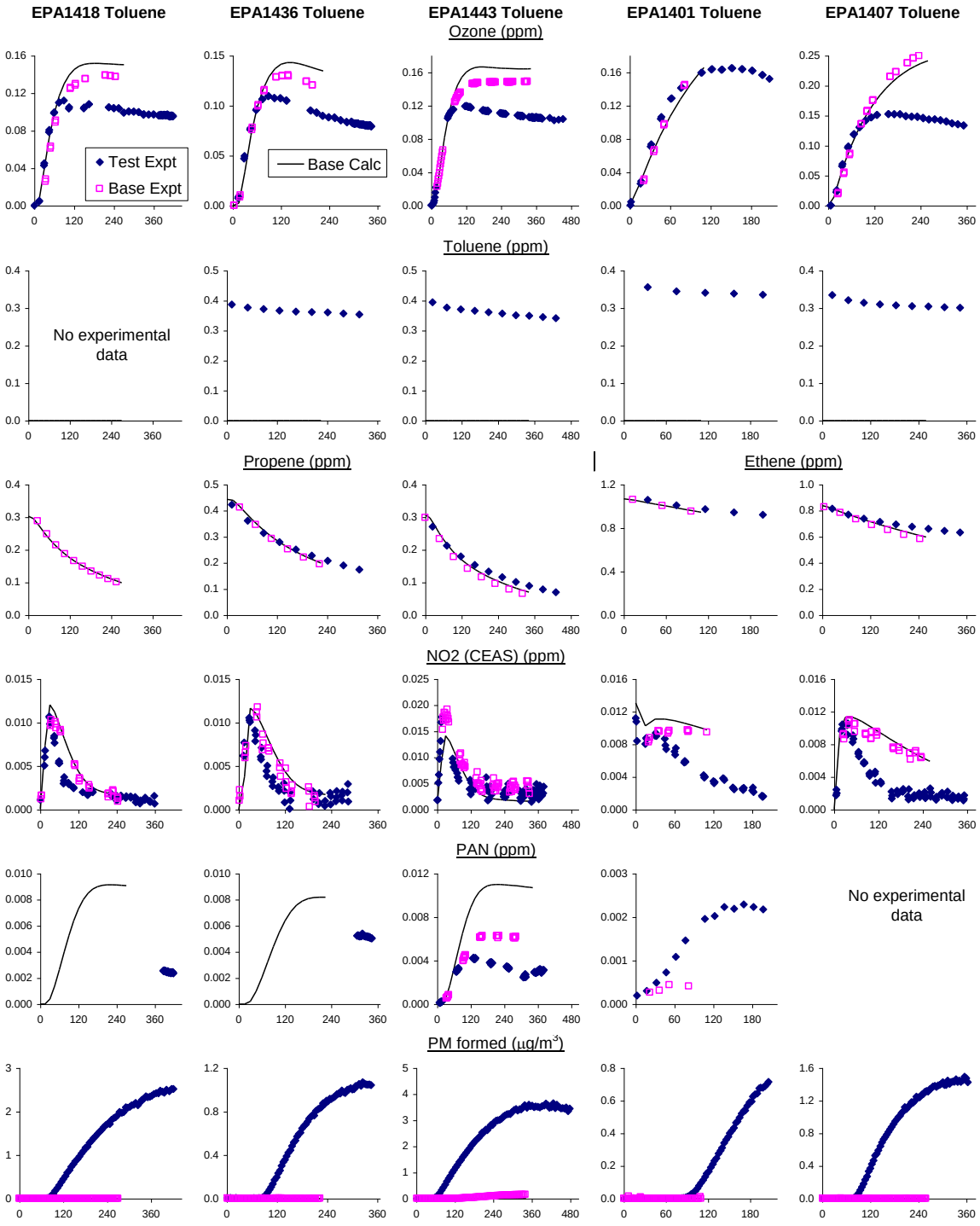

Figure 4- 3 Plots of selected results of NOx sink experiments with toluene. (Results of the model calculations

In all cases studied, it was found that the addition of the test compound caused a reduction in O_3 formation and it provides useful data for evaluating the effects of NO_x sinks on the maximum O_3. In terms of relative effects on O_3 reductions, which can be interpreted as relative strengths of NO_x sinks in the mechanisms of the compounds, the ordering is o-cresol > furan > toluene > isoprene. This is reasonably consistent with expectations, with the possible exception of furan, where the NO_x sink processes of the reactive unsaturated dicarbonyl formed (2-butene-1,4-dial) are highly uncertain. Only a few NO_x sink experiments had data for PAN. Because of lack of characterized experiments for thermodecomposition methods coupled with CEAS, the data for CEAS PAN is rejected. These experiments also provided data on secondary organic aerosol (SOA) formation from the reactions of the test compounds and their oxidation products, detail of which can also be found in the report of Texas Air Quality Research Program[15].

4.3.2 NO_x Source Experiments

NO_x source experiments were carried out with isopropyl and isobutyl nitrates and 2-nitrophenol, in all three cases using both VOC - acetaldehyde - H_2O_2 and VOC - CO - H_2O_2 irradiations. The concentration-time plots of NO_x source experiments with 2-nitrophenol is shown in Figure 4 - 1 as an example of one of the investigated systems. Data of other experiments can also be found in the report of Texas Air Quality Research Program[15].

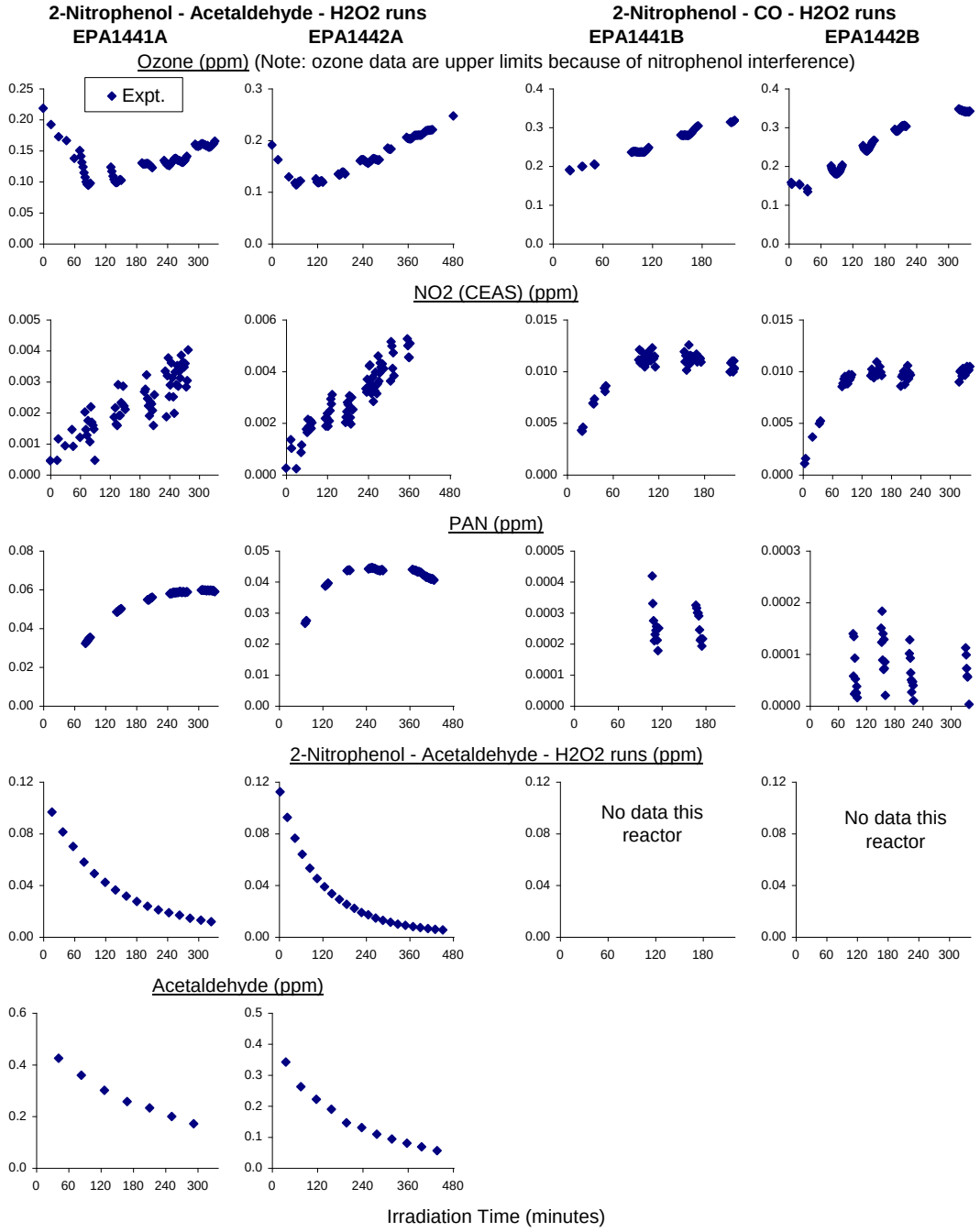

Figure 4- 4 Plots of selected results of NOx source experiments with 2-nitrophenol

The levels of NO_x species measured in the NO_x source experiments with the alkyl nitrate or nitrophenol test compounds were in all cases significantly higher then the measured NO_x species in the characterization experiments where the test compounds was absent. The amounts of O_3 formed in the experiments with the test compounds were also higher. Therefore, these experiments were successful in showing that these compounds indeed release measurable amounts of NO_x when they react. Usable CEAS NO_2 data are available from most of the experiments to show that the CEAS instrument was sufficiently sensitive to detect and quantify the NO_2 in the experiments. No valid GC-Luminol data were obtained for the isopropyl nitrate or the 2-nitrophenol experiments, but they were available in the experiments with isobutyl nitrate, and were sufficiently sensitive to quantify NO_2 in the acetaldehyde run. Thus these NO_2 data can serve as an additional means for mechanism evaluation when modeling at least some of the VOC - acetaldehyde - H_2O_2 experiments.

4.3.3 Other Single VOC - NO_x Control and Characterization Experiments

As part of this project, an ethene - NO_x and several propene - NO_x control experiments were also carried out, as well as a CO - NO_x characterization experiment to evaluate background chamber radical sources. In addition, three isoprene - NO_x experiments were carried out during the course of this project and useful data useful is obtained for mechanism evaluation. NO_2 data from both the CEAS and GC-Luminol instruments were in reasonably good agreement.

Data are also available for evaluation of mechanisms for SOA formation from those VOCs. Detailed analysis can be found in the report of Texas Air Quality Research Program and further discussion of this is beyond the scope of this thesis.

4.4 Conclusion

A sensitive and portable CEAS NO_2 detector has been developed and used in environmental chamber study for evaluating NO_x sinks and recycling, providing reliable and interference – free measurement of NO_2. 55 runs were conducted and analyzed with comparison to SAPRC-2007 model outputs. Information was obtained for evaluating model predictions of NO_x sinks in the atmospheric reactions of representative aromatics and aromatic oxidation products and in the reactions of isoprene, and for evaluating NO_x recycling processes involving reactions of representative oxidation products formed in the reactions of alkanes and aromatics. NO_x recycling from reactions was confirmed in experiments by CEAS where NO_2 were observed. The data of reactions of isoprene is also obtained for evaluating mechanisms for were also obtained. This project will provide a good basis for developing recommendations for improving chemical mechanisms used in regulatory applications.

.

Reference：

1. Jeffries, H.E.G., M.W.; and Carter, W.P.L, Protocol for evaluating oxidant mechanisms for urban and regional models. Report for U.S. Environmental Protection

Agency Cooperative Agreement No. 815779, Atmospheric Research and Exposure Assessment Laboratory, Research Triangle Park, NC. 1992.

2. Calvert, J.G., R. Atkinson, J. A. Kerr, S. Madronich, G. K. Moortgat, T. J. Wallington and G. Yarwood, The Mechanisms of Atmospheric Oxidation of Alkenes. Oxford University Press, New York., 2002.

3. Bierbach, A., I. Barnes, K. H. Becker, Product and Kinetic Study of the OH-Initiated Gas-Phase Oxidation of Furan, 2-Methylfuran and Furanaldehydes at ≈ 300 K. Atmos. Environ, 1995. **29**(19): p. 2651-2660.

4. Gómez Albarez, E., E. Borrás, J. Viidanoja, J. Hjorth, Unsaturated Dicarbonyl Products from the OH-Initiated Photo-oxidation of Furan, 2-Methlyfuran and 3-Methylfuran. Atmos. Environ, 2009. **43**: p. 1603-1612.

5. Engeln, R., G. Berden, R. Peeters, and G. Meijer, Cavity enhanced absorption and cavity enhanced magnetic rotation spectroscopy. Review of Scientific Instruments 1998. **69**(11): p. 3763-3769.

6. Paul, J.B., L. Lapson, and J. G. Anderson, Ultrasensitive absorption spectroscopy with a high-finesse optical cavity and off-axis alignment. Applied Optics, 2001. **40**(27): p. 4904-4910.

7. Fiedler, S.E., A. Hese, A. A. Ruth, Incoherent broad-band cavity-enhanced absorption spectroscopy. Chemical Physics Letters, 2003. **371**(284-294).

8. Langridge, J.M., S. M. Ball, and R. L. Jones (2006), A compact broadband cavity enhanced absorption spectrometer for detection of atmospheric NO2 using light emitting diodes. Analyst, 2006. **131**(916-922).

9. Washenfelder, R.A., A. O. Langford, H. Fuchs, and S. S. Brown Measurements of glyoxal using an incoherent broadband cavity enhanced absorption spectrometer. Atmospheric Chemistry and Physics, 2008. **8**: p. 7779-7793.

10. Burrows, J.P., A. Dehn, B. Deters, S. Himmelmann, A. Richter, S. Voigt and J. Orphal Atmospheric remote-sensing reference data from GOME: Part I. Temperature-dependent absorption cross-sections of NO2 in the 231-794 range. Journal of Quantitative Spectroscopy & Radiative Transfer, 1998. **60**(6): p. 1025-1031.

11. Singh, T., R. F. Sawyer, E. S. Starkman, and L. S. Caretto Rapid continuous determination of nitric oxide concentration in exhaust gases. Journal of the Air Pollution Control Association, 1968. **18**(2): p. 102-105.

12. Fried, A., and J. Hodgeson, Laser photoacoustic detection of nitrogen dioxide in the gas-phase titration of nitric oxide with ozone,. Anal. Chem, 1982. **54**(2): p. 278-282.

13. Bertram, T.H., R. C. Cohen, W. J. Thorn III and P. M. Chu (2005), Consistency of ozone and nitrogen oxides standards at tropospherically relevant mixing ratios. Journal of the Air & Waste Management Association, 2005. **55**(10): p. 1473-1479.

14. Day, D.A., P. J. Wooldridge, M. B. Dillon, J. A. Thornton, and R. C. Cohen A thermal dissociation laser-induced fluorescence instrument for in situ detection of NO2, peroxy nitrates, alkyl nitrates, and HNO3,. Journal of Geophysical Research, 2002. **107**.

15. Heo, W.P.L.C.a.G., Sinks and Recycling in Atmospheric Chemical Mechanisms: Technical Memorandum on Experiments. Texas Air Quality Research Program, 2011. Project No. 10-052

Chapter 5 In situ detection of gas phase glyoxal for SOA formation in environmental chamber study using CEAS

5.1 Introduction.

Glyoxal (CHOCHO) is the smallest α-dicarbonyl type compound. It is formed in the atmosphere during the oxidation of hydrocarbons, which are emitted by biogenic and anthropogenic sources. In particular, glyoxal is an important ring-cleavage product in the OH-radical initiated oxidation of aromatic hydrocarbons [1, 2], and is also formed in the reaction of O_3 and OH-radicals with some alkenes[3-5] and unsaturated aliphatic oxygenated hydrocarbons[6, 7]. Therefore, glyoxal is a molecule of emerging importance to the atmospheric chemistry community due to its role in aerosol formation and as an indicator for oxidative chemistry.

The glyoxal fate in troposphere is largely determined by its photolysis and reaction with OH-radicals[8, 9]. Photolysis of glyoxal leads to the formation of H2, CO, HCHO and HCO radicals and it is also a significant source of HOx (OH+HO2)[10-12]. Atmospheric residence time with respect to photolysis is limited during the day to a few hours [8]. Possibly nighttime reaction with NO_3 radicals is another removal pathway of tropospheric glyoxal.

In addition, glyoxal also plays an important role in the formation of secondary organic aerosol (SOA) in the atmosphere [13-16]. Reactive uptake of glyoxal on aqueous

seed aerosol may lead to significant particle growth [15]. A field study in Mexico City shows that the atmospheric budget of glyoxal can not be balanced without an aerosol loss process[17]. Despite glyoxal SOA formation studies, further quantification of SOA yields as a function of conditions such as relative humidity, irradiation, gas phase glyoxal mixing ratio, and seed aerosol composition are required in order to allow for the application of laboratory findings to ambient conditions. Glyoxal is also promising as a model surrogate for compounds that can yield SOA via formation, condensation, and photochemical reactions. Therefore, environmental study of glyoxal is very important for better understanding the role glyoxal played in atmosphere.

Atmospheric measurements of glyoxal are scarce, but tropospheric mixing ratios have been reported to range between several 100 ppt to few ppb[18]. Good simulation chamber experiment requires studying comparable concentration of glyoxal. Therefore, a sensitive, accurate, fast, portable, real time and in stu measurement of glyoxal is highly desirable for field study and environmental chamber study. However, conventional methods for glyoxal measurement are chromatography methods which involve long sampling time and they are not online for direct measurement for gas phase glyoxal.

Compared to these wet chemistry methods, spectroscopic techniques provide direct and in situ measurement of glyoxal. Volkamer et al. (2005a)[19] demonstrated long path differential optical absorption spectroscopy (DOAS) in Mexico City to detect glyoxal by its structured absorption in the 420–465 nm spectral region, for an atmospheric path length of 4420m and integration times between 2 to 15 min, with a detection limit of 150 pptv. Although this method is reasonable for ambient measurement, it is not practical for chamber studies. Huisman et al. (2008)[20] recently demonstrated a laser-induced

phosphorescence technique, by exciting glyoxal at 440.25 nm using a tuned Ti:sapphire laser and observing the phosphorescence at 520 nm. This instrument has excellent sensitivity for 18ppt/1min. It is a spatial, selective, sensitive, in situ technique for field and chamber study, but the instrument is relatively expensive. Another technique that has considerable potential for sensitive and specific measurement of glyoxal is incoherent broadband CEAS[21]. CEAS is an excellent detection method for atmospheric trace gases with broad, structured absorptions in the visible and ultraviolet spectral regions, and is particularly useful for simultaneously determining the concentration of molecules with significant spectral overlap, such as CHOCHO and NO_2. Recently, S. S. Brown and his coworkers reported the first laboratory measurements of CHOCHO by CEAS, together with simultaneous measurements of NO_2[22]. For a 1-min sampling time, the precision ($\pm 1\sigma$) on signal for measurements of CHOCHO and NO_2 is 29 pptv and 20 pptv, respectively. In this project, an instrument was built based on S. S. Brown‘s work with the notable exception of a much smaller and cheaper LED as the light source. (Brown et al., used a 75W Xe arc lamp, which required cooling housing, cold window and optical filters). Our CEAS instrument was installed in the CE-CERT UCR/EPA chamber to study the behavior of glyoxal in atmospheric chemistry and SOA formation.

This project is the first environment chamber study of glyoxal using CEAS to directly measure glyoxal uptaken to study its SOA formation. It is also the first paper to report direct measurement of gas phase glyoxal production from aromatic VOCs and isoprene using CEAS.

5.2 Experimental

The detail description of CEAS instrument and its principle can be found in Chapter 2; in addition, since this instrument is also used for NO2 detection in other projects, the specific description for NO_2/glyoxal CEAS instrument has been discussed in chapter 4.

For the data acquisition, we used the same NO_2 Labview fitting program described in Chapter 4 to extract glyoxal reading. Instead of extracting $n_{NO2,}$ $n_{glyoxal}$ was extracted from a fitted polynomial equation (eqn (4.2)). The glyoxal absorption crosssection in the 445-455nm range was obtained from Volkamer's work[19]. Similar to NO_2 detection, a smaller range (446.5 nm to 450.0 nm) was used for raw data fitting to minimize interferences from other trace species while utilizing only the strongest glyoxal absorption peak. From the Labview program, the number density of glyoxal can be first calculated and then coverted into parts-per-billion by using idea gas law, while the NO_2 concentration can be obtained simultaneity. The detailed data acquisition description is found in Chapter 4.

All experiments for this project were carried out in an indoor environmental chamber with blacklights as the light source. The detailed description and characterizations of UCR/CE-CERT chamber and related instruments for this projected can be found in chapter 2.

Synthesis of glyoxal followed the method outlined by Frank Keutsch [23]. In general, glyoxal was prepared by heating a mixture of solid glyoxal trimer dehydrate (Sigma, minimum 97%) and phosphorus pentoxide (P_2O_5) to ~160 ℃ under vacuum. The monomer was collected in an LN_2 trap as a yellow solid and stored overnight at −20°C. Prior to each experiment, the frozen monomer was allowed to vaporize into a 500mL

glass bulb and introduced into the chamber using a gentle N_2 stream. AS (ammonia sulfate) seed particles were generated by atomization of a 0.015M aqueous AS solution using a constant rate atomizer.

Before each experiment the reactors were thoroughly flushed with dry purified air and filled to their maximum volume. Common reactants for both reactors were simultaneously injected and then mixed. Once reactant levels stabilized and initial reactant concentrations determined, the irradiations commenced by turning on the lights. Sampling was conducted alternatively or simultaneously from both reactors during the irradiation. The experiments ended after about 8 hours or when both reactors were depleted and simultaneous measurements were carried out.

This project includes two parts for glyoxal study. The first part is to study the glyoxal uptaken through oligomer formation and by aqueous aerosol, while the second part is to understand the glyoxal formation from the photooxidation of aromatic hydrocarbons in atmosphere and oxidation product of isoprene.

The 8 glyoxal uptake experiments and 16 experiments of glyoxal formation are summarized in Table 5- 1 and Table 5- 2.

Table 5- 1 Summary of glyoxal uptaken experiments for this project.

Run	Run type	RH(%)	Seed type	Seed vol, initial (μm3/cm3)	GL CEAS Ini Concentration (ppb)
1359	GL wall loss	61-54	No		73
1360	GL wall loss	57-55	no/AS		72
1361	GL uptake onto AS	58-55	AS	10	81
1362	GL wall loss	72-69	No		26
1363	GL wall loss	76-71	No		61
1365	GL wall loss → dilution	51-53	No		75
1368	GL uptake onto AS	73-72	AS	74	52
1371	GL uptake onto AS	0	AS	19	79

（GL=glyoxal; AS= $(NH_4)_2SO_4$）

Table 5- 2. Summary of glyoxal formation experiments for this project.

Run ID	Type	Time	Temp.	Dilution	Test Reactant		Initial Concentrations (ppm)							
		(min)	(K)	(min-1)	Compound	(ppm)	NO	NO_2	H_2O_2	CO	Ethene	Propene	Acetald.	Tracer
	NOx Sink Experiments													
EPA1401A	Toluene - Ethene - NO_x	207	298.8	-	Toluene	0.367	0	0.013			1.1			0.073
EPA1401B	Ethene - NO_x	110	298.8	-			0	0.013			1.07			0.075
EPA1407A	Toluene - Ethene - NO_x	363	298.8	2.00E-05	Toluene	0.344	0.014	0			0.84			0.05
EPA1407B	Ethene - NO_x	259	298.8	-			0.014	0			0.84			0.05
EPA1418A	Toluene - Propene - NO_x	421	298.2	-	Toluene	0.301	0.016	0				0.303		0.075
EPA1418B	Propene - NO_x	270	298.2	3.00E-05			0.015	0				0.303		0.075
EPA1436A	Toluene - Propene - NO_x	348	298.1	5.00E-05	Toluene	0.391	0.014					0.431		0.104
EPA1436B	Propene - NO_x	225	298.1	2.00E-05			0.014					0.443		0.106
EPA1443A	Toluene - Propene - NOx	481	298	-	Toluene	0.407	0.017	0.001				0.305		
EPA1443B	Propene - NOx	342	298	-			0.017	0.001				0.307		
EPA1444A	Isoprene - Ethene - NO_x	509	298.1	-	Isoprene	0.017	0.014	0			0.8			
EPA1444B	Isoprene - Ethene - NO_x	252	298.1	-	Isoprene	0.017	0.014	0			0.8			
EPA1446A	Isoprene - Ethene - NO_x	369	298.5	-	Isoprene	0.05	0.001	0.013			0.92			
	Isoprene Experiments													
EPA1397A	Isoprene - NO_x	477	299.6	2.00E-05	Isoprene	0.25	0.024							0.078
EPA1405A	Isoprene - NO_x	326	299	-	Isoprene	0.192	0.016							0.072
EPA1405B	Isoprene - NO_x	207	299	-	Isoprene	0.2	0.006							0.075

5.3 Results and discussion.

5.3.1 Glyoxal uptake through oligomer formation and by aqueous aerosol.

All glyoxal uptake experiments were conducted under dark reaction conditions. Two glyoxal uptake systems were studied, including (1) wall loss of glyoxal under dry and humid conditions and (2) glyoxal uptaken by inorganic seed (AS) under dry and humid conditions.

5.3.1.1 Glyoxal chamber wall loss under humid condition.

Table 5-1 shows the glyoxal uptake experiments list and their conditions for all the experiments in our chamber. Under dry conditions, no glyoxal wall loss was observed. Similarly, for relative humidity (RH) up to 50%, observed glyoxal wall loss were not observed.

When the RH level is between 50% and 60%, measureable glyoxal wall loss was sometimes observed. For example, Figure 5-1 indicated that with 60% RH in the chamber, no wall loss can be observed. In this figure, at around 200 min, the chamber started to be diluted and both of the glyoxal concentration and tracer concentration decrease at a same rate.

When the RH level is above 70%, significant glyoxal wall loss can be observed and the results are repeatable, which is shown in Figure 5-2. This phenomena indicates that

reaction chamber wall loss rate of glyoxal was observed to be strongly dependent on RH, with RH of 50~60% being a threshold for significant glyoxal chamber wall loss. Similar conclusion were also obtained for the Caltech chamber[24]. In the experiment where significant wall loss can be observed, the decrease of glyoxal is slower than that of tracer when the chamber is diluted, indicating the wall acts as a glyoxal reservoir.

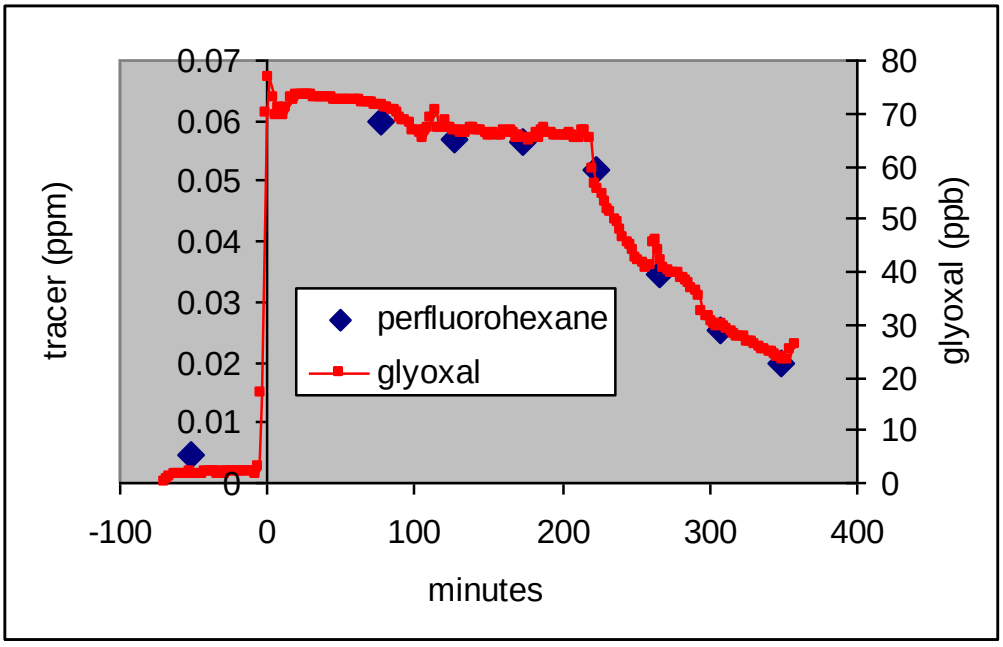

Figure 5- 1 time dependence of glyoxal and tracer (perfluorohexane) concentration under 60% RH. At time 200 min, the chamber started to be diluted.

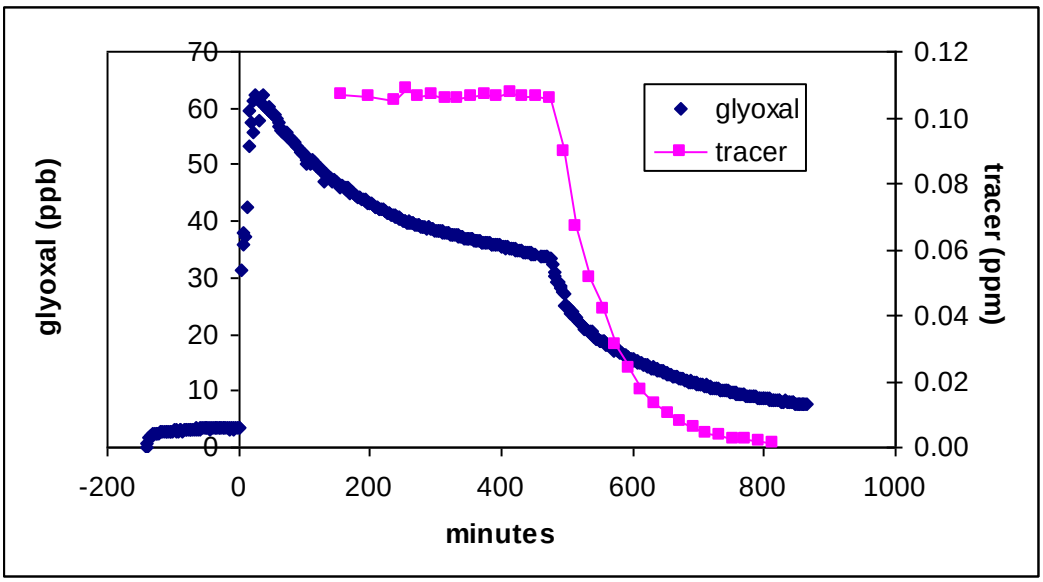

Figure 5- 2 time dependence of glyoxal and tracer (perfluorohexane) concentration under 70% RH. At time 480 min, the chamber started to be diluted. Decrease of glyoxal is slower than that of tracer, indicating the wall acted as reservoir of glyoxal.

5.3.1.2 Glyoxal uptake by inorganic seed (AS) under dry and humid conditions.

Similarly to glyoxal wall loss experiments, RH between 50% and 60% becomes a threshold for significant glyoxal uptake onto inorganic AS seed. AMS data indicated that no contribution to SOA formation from glyoxal is observed under dry conditions (RH <1%) and minor contributions from glyoxal to SOA formed under elevated humidity (RH~60%), even with the presence of OH radical source and seed particles.

RH bigger than 70% can cause significant SOA formation by glyoxal uptaking onto AS. Figure 5-3 indicated that when RH is 73%, glyoxal is significantly removed by wet AS seed while the AMS organic increased after glyoxal injection, indicating SOA formation from glyoxal uptake onto AS seed.

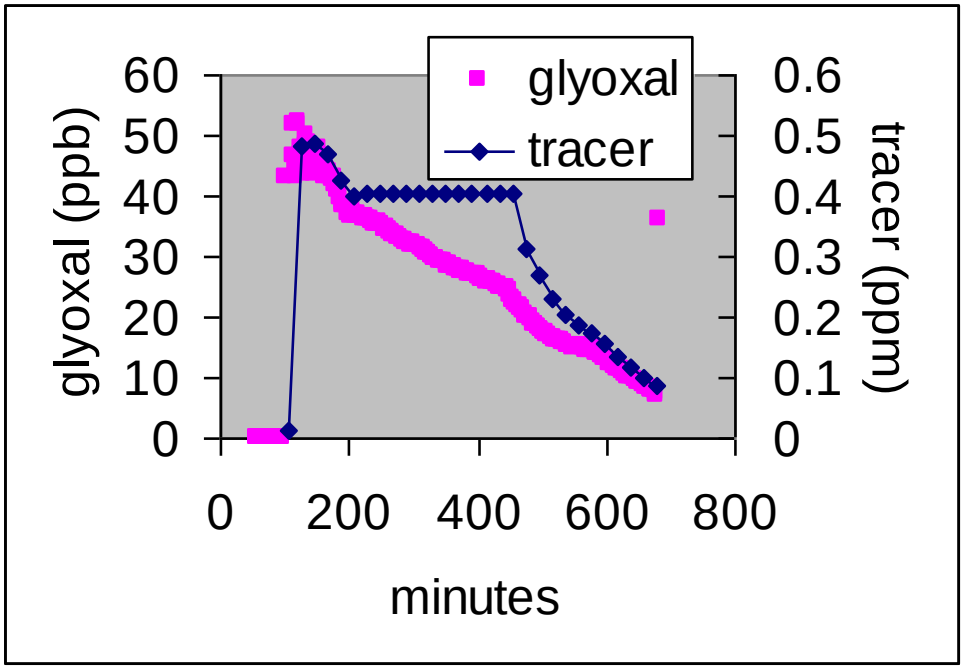

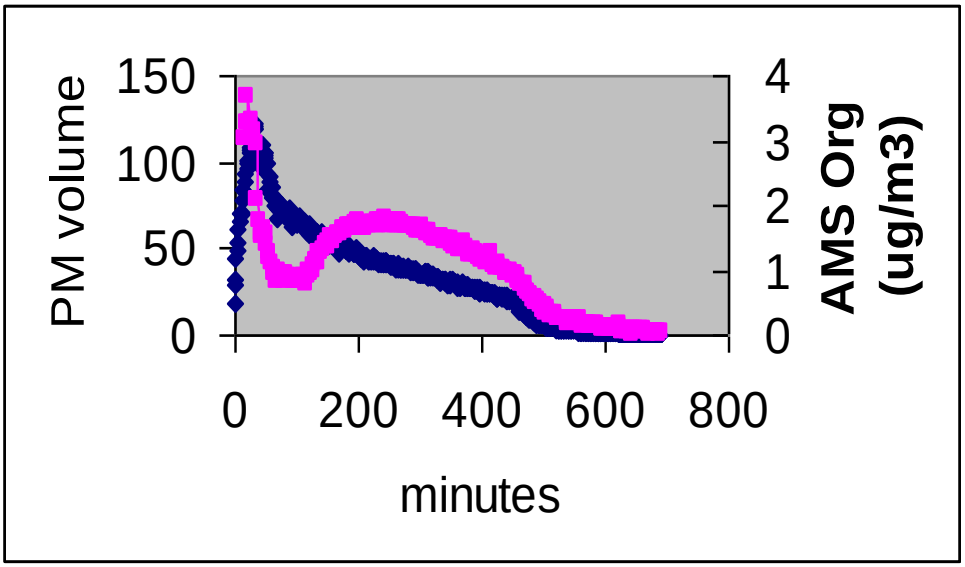

Figure 5- 3 time dependence for glyoxal uptaking onto AS under 73% RH. (1) Time dependence of glyoxal and tracer (perfluorohexane) concentration. At time 450 min, the chamber started to be diluted. (2). Time evolution of SOA using PM volume and AMS data. AMS organic increased after glyoxal injection, indicating SOA formation from glyoxal uptake onto AS seed.

In summary, our experiments demonstrated that high RH impacts significantly on glyoxal chamber wall loss and glyoxal uptaken by AS seed. Reaction chamber wall loss rate of glyoxal was observed to be strongly dependent on RH, with RH of 50~60% being a threshold for significant glyoxal chamber wall loss. However, compared to pervious work[24], our threshold is much higher and minor contributions from glyoxal to SOA formed under elevated humidity (RH~60%), even with the presence of OH radical source and seed particles. No contribution to SOA formation from glyoxal is observed under dry conditions (RH <1%).

5.3.2 Glyoxal formation from the photooxidation of toluene and isoprene

The experimental conditions for glyoxal formation from the photooxidation of toluene and isoprene are listed in table 5-2. Toluene was chosen as a representative aromatic hydrocarbon that is important in emissions and is known to have large glyoxal yields[25]. Isoprene is an important biogenic compound that dominates emissions in many non-urban and some urban areas. Therefore, although the glyoxal production yield for isoprene is not as big, the overall atmospheric effect is dramatic. Besides the test reactants VOCs, ethene and propene are also chosen as control experiments to evaluate the base case experiments, and to assure that equivalent results are obtained in simultaneous irradiations in each of the dual reactors if the same mixtures are irradiated. It is also important to assure that the base case experiment can be adequately be simulated by current mechanisms for them to be useful for evaluating mechanisms for the effects of adding the test compound.

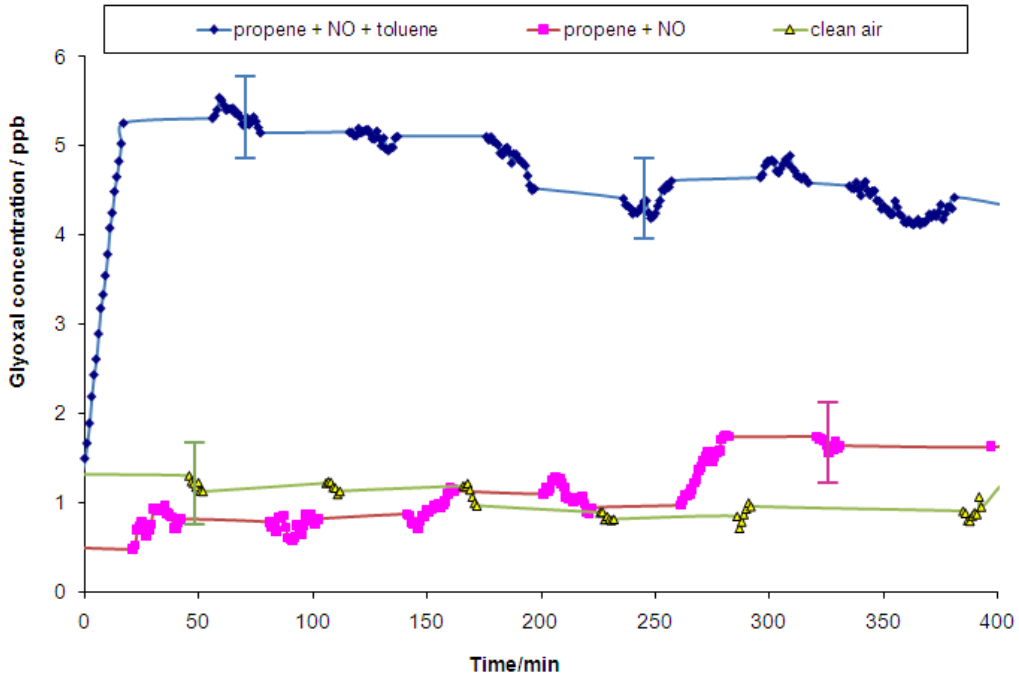

Figure 5- 4 Time dependence curve for Toluene - Propene - NOx glyoxal production. The siganl is switching between Toluene - Propene – NOx system and Propene – NOx. The difference between these two level is the glyoxal formation from toluene reaction.

Figure 5-4 shows an example of the glyoxal formation from Toluene - Propene – NOx system. In this experiment, propene reacts as a base case experiment while the therotical glyoxal formation from propene – NOx system can be negligible. When operating this experiment, the siganl is switching between Toluene - Propene – NOx system and Propene – NOx system. The difference between these two level is the glyoxal formation from toluene reaction. From this experiment, the generated glyoxal is about 4ppb and its production yield from this toluene system is 26% which is comparetable to literature results, which is ~20%[26].

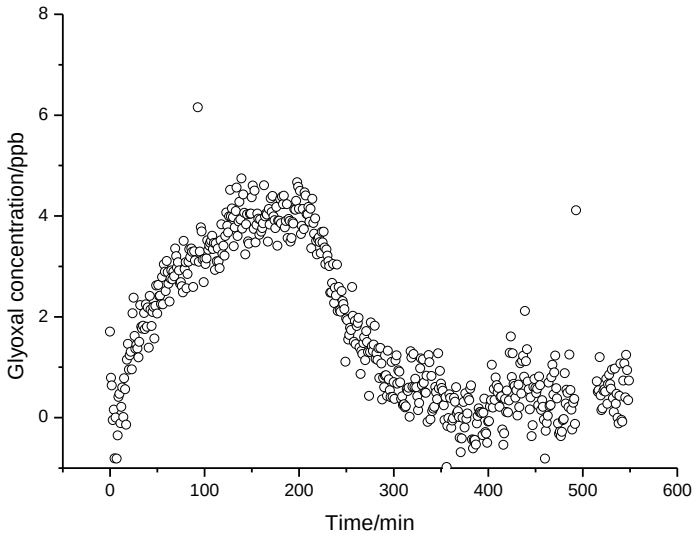

Figure 5- 5 Time dependence curve for Isoprene - NOx glyoxal production.

Glyoxal formation from isoprene – NOx result is shown in Figure 5-5. The maximum production of glyoxal is about 4.5ppb, which is equal to 4.5% glyoxal yield, where about 0.1 ppm isoprene reacted. This result is similar to Galloway's recent work[27]. The decrease of glyoxal after 9:36 might due to glyoxal removal by photolysis, which requires additional analysis of other instrumental data alsoconnected to our chamber.

5.4 Conclusion

Glyoxal is one of the major products from many classes of biogenic and anthropogenic compounds in the atmosphere and it is reported to contribute to SOA formation through oligomer formation. SOA formation from glyoxal with the presence of inorganic seed (AS) under varied humidity is evaluated in this study. Preliminary results

indicate minor contributions from glyoxal to SOA formed under elevated humidity (RH~60%), even with the presence of OH radical source and seed particles. Significant contribution to SOA formation from glyoxal is observed only under wet conditions (RH > 60%). Reaction chamber wall loss rate of glyoxal was observed to be strongly dependent on RH, with RH of 50~60% being a threshold for significant glyoxal chamber wall loss. Furthermore this study also evaluated the role of glyoxal in SOA formation from the photooxidation of toluene and isoprene using the environmental chamber at UCR/CE-CERT. This project is the first to report glyoxal formation from VOCs using in-situ CEAS glyoxal measurements. The results are comparable to literature glyoxal yield results. Besides the glyoxal CEAS data, data from other instruments are available for further analysis. Further chemical mechanism is explored using a suite of off-line and on-line techniques such as liquid chromatography – time-of-flight mass spectrometry (LC-ToF) and Aerodyne high-resolution time-of-flight aerosol mass spectrometry (HR-ToF-AMS), which is beyond the work of this thesis.

Reference

1. Volkamer, R., U. Platt, and K. Wirtz, *Primary and secondary glyoxal formation from aromatics: Experimental evidence for the bicycloalkyl-radical pathway from benzene, toluene, and p-xylene.* Journal of Physical Chemistry A, 2001. 105(33): p. 7865-7874.

2. Smith, D.F., T.E. Kleindienst, and C.D. McIver, *Primary Product Distributions from the Reaction of OH with m-, p-Xylene, 1,2,4- and 1,3,5-Trimethylbenzene.* Journal of Atmospheric Chemistry, 1999. 34(3): p. 339-364.

3. Hatakeyama, S., N. Washida, and H. Akimoto, *Rate constants and mechanisms for the reaction of hydroxyl (OD) radicals with acetylene, propyne, and 2-butyne in air at 297 .+-. 2 K.* The Journal of Physical Chemistry, 1986. 90(1): p. 173-178.

4. Grosjean, D., *Gas-phase reaction of ozone with 2-methyl-2-butene: dicarbonyl formation from Criegee biradicals.* Environmental Science & Technology, 1990. 24(9): p. 1428-1432.

5. Martinez, R.I. and J.T. Herron, *Stopped-flow studies of the mechanisms of ozone-alkene reactions in the gas phase: trans-2-butene.* The Journal of Physical Chemistry, 1988. 92(16): p. 4644-4648.

6. Magneron, I., et al., *A Study of the Photolysis and OH-initiated Oxidation of Acrolein and trans-Crotonaldehyde.* The Journal of Physical Chemistry A, 2002. 106(11): p. 2526-2537.

7. Grosjean, E. and D. Grosjean, *The Reaction of Unsaturated Aliphatic Oxygenates with Ozone.* Journal of Atmospheric Chemistry, 1999. 32(2): p. 205-232.

8. Plum, C.N., et al., *Hydroxyl radical rate constants and photolysis rates of .alpha.-dicarbonyls.* Environmental Science & Technology, 1983. 17(8): p. 479-484.

9. Klotz, B., et al., *A kinetic study of the atmospheric photolysis of α-dicarbonyls.* International Journal of Chemical Kinetics, 2001. 33(1): p. 9-20.

10. Langford, A.O. and C.B. Moore, *REACTION AND RELAXATION OF VIBRATIONALLY EXCITED FORMYL RADICALS.* Journal of Chemical Physics, 1984. 80(9): p. 4204-4210.

11. Zhu, L., D. Kellis, and C.F. Ding, *Photolysis of glyoxal at 193, 248, 308 and*

351 nm. Chemical Physics Letters, 1996. 257(5-6): p. 487-491.

12. Chen, Y.Q. and L. Zhu, *Wavelength-dependent photolysis of glyoxal in the 290-420 nm region.* Journal of Physical Chemistry A, 2003. 107(23): p. 4643-4651.

13. Hastings, W.P., et al., *Secondary organic aerosol formation by glyoxal hydration and oligomer formation: Humidity effects and equilibrium shifts during analysis.* Environmental Science & Technology, 2005. 39(22): p. 8728-8735.

14. Jang, M.S., et al., *Heterogeneous atmospheric aerosol production by acid-catalyzed particle-phase reactions.* Science, 2002. 298(5594): p. 814-817.

15. Kroll, J.H., et al., *Chamber studies of secondary organic aerosol growth by reactive uptake of simple carbonyl compounds.* Journal of Geophysical Research-Atmospheres, 2005. 110(D23).

16. Liggio, J., S.-M. Li, and R. McLaren, *Reactive uptake of glyoxal by particulate matter.* Journal of Geophysical Research, 2005. 110(D10304).

17. Volkamer, R., et al., *A missing sink for gas-phase glyoxal in Mexico city: Formation of secondary organic aerosol.* Geophysical Research Letters, 2007. 34(L19807).

18. Grosjean, E., et al., *Air Quality Model Evaluation Data for Organics. 2. C1−C14 Carbonyls in Los Angeles Air.* Environmental Science & Technology, 1996. 30(9): p. 2687-2703.

19. Volkamer, R., et al., *High-resolution absorption cross-section of glyoxal in the UV-vis and IR spectral ranges.* Journal of Photochemistry and Photobiology a-Chemistry, 2005. 172(1): p. 35-46.

20. Huisman, A.J., et al., *Laser-induced phosphorescence for the in situ detection*

of glyoxal at part per trillion mixing ratios. Analytical Chemistry, 2008. 80(15): p. 5884-5891.

21. Fiedler, S.E., A. Hese, A. A. Ruth, *Incoherent broad-band cavity-enhanced absorption spectroscopy.* Chemical Physics Letters, 2003. 371(284-294).

22. Washenfelder, R.A., A. O. Langford, H. Fuchs, and S. S. Brown *Measurements of glyoxal using an incoherent broadband cavity enhanced absorption spectrometer.* Atmospheric Chemistry and Physics, 2008. 8: p. 7779-7793.

23. Galloway, M.M., et al., *Glyoxal uptake on ammonium sulphate seed aerosol: reaction products and reversibility of uptake under dark and irradiated conditions.* Atmos. Chem. Phys. Discuss., 2008. 8(6): p. 20799-20838.

24. Loza, C.L., et al., *Characterization of Vapor Wall Loss in Laboratory Chambers.* Environmental Science & Technology, 2010. 44(13): p. 5074-5078.

25. Tuazon, E.C., R. Atkinson, C. N. Plum, A. M. Winer, and J. N. Pitts, Jr. , *The Reaction of Gas-Phase N2O5 with Water Vapor.* Geophys. Res. Lett. , 1983. 10(953-956).

26. Nishino, N., J. Arey, and R. Atkinson, *Formation Yields of Glyoxal and Methylglyoxal from the Gas-Phase OH Radical-Initiated Reactions of Toluene, Xylenes, and Trimethylbenzenes as a Function of NO2 Concentration.* The Journal of Physical Chemistry A, 2010. 114(37): p. 10140-10147.

27. Galloway, M.M., et al., *Yields of oxidized volatile organic compounds during the OH radical initiated oxidation of isoprene, methyl vinyl ketone, and methacrolein under high–NOx conditions.* Atmos. Chem. Phys. Discuss., 2011. 11(4): p. 10693-10720.

Chapter 6 Conclusion

Air pollution and global climate change are important environmental issues that affect our society. To understand these problems and to develop control strategies requires deeper understanding of atmospheric chemistry, which seeks to reveal the causes of these problems and to evaluate possible solutions and government policies.

Environmental chambers have been used for the past few decades to study atmospheric chemistry and investigate processes leading to secondary pollutant formation such as ozone[1] and secondary organic aerosol (SOA)[2]. Environmental chambers are essential for developing and evaluating chemical mechanisms or models for understanding the important mechanisms of atmospheric chemical reactions and predicting the formation of secondary pollutants in the absence of uncertainties associated with emissions, meteorology, and mixing effects.

A good environmental chamber should have the capability to simulate the real ambient conditions, which requires specialized, sensitive and real time instruments to detect important reactants and/or products. This thesis work provides two different high sensitivity real time instruments to detect NO_3 and NO_2/ glyoxal for environmental chamber study.

The instruments were demonstrated to be useful for detection of trace gas phase species based on absorption spectroscopy, utilizing ~660 nm for NO_3 detection and ~450 nm for NO_2/glyoxal detection. The sensitivities are for 10 ppt/2min for NO_3, ~1ppb/1min for NO_2 and ~1.5 ppb/min for glyoxal under the chamber sampling conditions. With the small and

economical LEDs as the light sources, portable analyzers for NO_3 and NO_2 are constructed. Data continue to be collected in the UCR/CE-CERT chamber for studying important chemistry of NO_3 NO_2, and glyoxal.

In the NO_3 project, direct measurement of NO_3 radical has been carried out in our environmental chamber. The production of NO_3 is observed directly from the reaction between NO_2 and O_3. The NO_3 decay from injecting of N_2O_5 under dry and humid conditions has been characterized. In addition, the relative reaction rate of NO_3 and amine reactions is also obtained.

The NO_2 project of my thesis work is also a very important part of Texas Air Quality Research Program. In this project, many chamber experiments were carried out to evaluate model predictions of O_3 formation and sources and sinks for oxides of nitrogen (NO_x) in the atmospheric photooxidation reactions of representative compounds. These experiments confirmed the presence of NO_x recycling processes in the reactions of these compounds.

In addition, the same NO_2 CEAS instrument is used for glyoxal uptake and formation studies. SOA formation from glyoxal with the presence of inorganic seed (AS) under varied humidity is evaluated in this study. Results indicate that significant contribution to SOA formation from glyoxal is observed only under wet conditions (RH > 60%). Furthermore this study also evaluated the role of glyoxal in SOA formation from the photooxidation of toluene and isoprene with comparable results to literature.

Overall, environmental chamber studies using CEAS measurement for important gas phase atmospheric species are characterized and new information of atmospheric chemistry is obtained from these projects, which can provide insightful data in atmospheric processes

and lead to a better understanding of the atmospheric system, which can eventually extend to environmental policy.

Reference

1. Carter, W.P.L., et al., *A new environmental chamber for evaluation of gas-phase chemical mechanisms and secondary aerosol formation.* Atmospheric Environment, 2005. **39**(40): p. 7768-7788.

2. Seinfeld, J.H. and J.F. Pankow, *Oranic atmospheric particulate material* Annual Review of Physical Chemistry, 2003. **54**(1): p. 121-140.